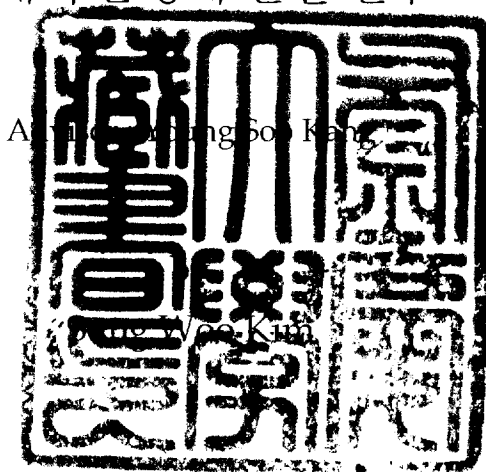


Preparation of MPS (mercaptopropyl  
trimethoxysilane) Coated-SiO<sub>2</sub>  
Nanoparticles and Effect on Mechanical  
Properties of EVA/SiO<sub>2</sub> Nanocomposite

MPS (mercaptopropyl trimethoxysilane) 코팅된  
SiO<sub>2</sub> 나노입자의 제조와 EVA/SiO<sub>2</sub> 나노복합체의  
기계적 물성에 관한 연구



A thesis submitted in partial fulfillment of the requirements  
for the degree of

Master of Science

in Department of Chemistry, The Graduate School,  
Pukyong National University

February, 2005

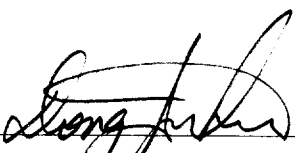
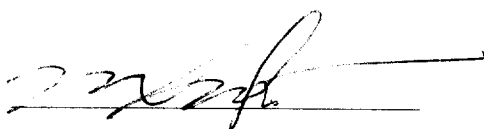
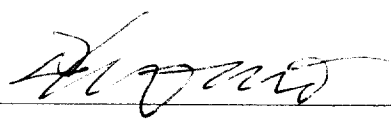
Preparation of MPS (mercaptopropyl trimethoxysilane)  
Coated-SiO<sub>2</sub> Nanoparticles and Effect on Mechanical Properties  
of EVA/SiO<sub>2</sub> Nanocomposite

A Dissertation

by

Sung Woo Kim

Approved as to style and content by :

  
Chair man : Dong Jae Lee  
Member : Young Soo Kang  
Member : Sung Doo Moon

February, 2005

## PART I

### Preparation of MPS (mercaptopropyl trimethoxysilane) Coated-SiO<sub>2</sub> Nanoparticles and Effect on Mechanical Properties of Surface Treated- SiO<sub>2</sub>/EVA Nanocomposite

김 성 우

부경대학교 대학원 화학과

#### 요 약

SiO<sub>2</sub> 나노입자는 TEOS (tetraethyl orthosilicate), sodium metasilicate 와 sodium silicate 로부터 합성되었다. SiO<sub>2</sub> 나노입자와 EVA (ethylene vinylacetate)와의 상용성과 분산성을 극대화 시키기 위해 실란 커플링제의 한 종류인 MPS (3-mercaptopropyl trimethoxysilane)으로 SiO<sub>2</sub> 나노입자를 표면코팅하였다. 나노입자의 형태와 분산성은 투과전자현미경(TEM), 주사전자현미경(SEM)으로 관찰하였고 나노입자의 표면코팅으로 인한 구조변화 및 성공적인 코팅을 푸리에변환 적외선분광분석기로 확인하였다. EVA/나노입자 복합체의 분산성은 광학사진으로 분석하였다. 최종적으로 EVA 와 표면개질 된 SiO<sub>2</sub> 나노입자와의 나노 복합체를 제조하여 내마모성, 경도, 인장강도와 신율 등의 기계적 특성을 조사하였다. EVA 에 SiO<sub>2</sub> 나노입자가 도입됨으로 인해 내마모성과 경도는 현저하게 증가하였지만, 인장강도와 신율에 있어서는 미비한 감소가 있었다.

## PART II

### Preparation of Heat Insulating Nanocomposite Film with MPS (mercaptopropyl trimethoxysilane) coated-Nanoparticles

김 성 우

부경대학교 대학원 화학과

#### 요 약

농업용 필름의 한가지 기능은 야간에 지면으로부터 방사되는  $7\ \mu\text{m} \sim 10\ \mu\text{m}$ 의 파장대를 가지는 방사에너지(열)를 흡수하는 것이다. 보온필름은 방사열을 흡수하여 주간과 야간의 비닐하우스 내부의 온도차이를 최소화하여 냉해를 방지해야 한다. 농업용 필름에 보온성을 부여하기 위해 보온성 filler로써  $\text{SiO}_2$ ,  $\text{Al}_2\text{O}_3$ ,  $\text{MgO}$  와  $\text{CaO}$  나노입자를 합성하였고, EVA (ethylene vinylacetate) 와 나노입자와의 상용성 및 분산성을 극대화하기 위해 MPS (mercaptopropyl trimethoxysilane)로 나노입자의 표면을 개질시켜 나노입자의 표면에 고분자와 결합을 이룰 수 있는 관능기를 도입하였다. EVA에 나노입자를 2 wt%의 중량비로 혼합하여 펠렛타이저에서 마스터배치를 제조한 후 Blow Film Extruder를 이용하여  $60\ \mu\text{m}$  두께의 필름을 제조하였다. 보온성 무기filler ( $\text{SiO}_2$ ,  $\text{Al}_2\text{O}_3$ ,  $\text{MgO}$  와  $\text{CaO}$  나노입자)를 함유한 EVA 필름의 분산성은 광학현미경으로 관찰하였고, 광 투과도는 자외선-가시광선 분광분석기로 분석하였다. 보온성은 간접적인 방법으로 적외선 분광분석기로  $700\ \text{cm}^{-1} \sim 1400\ \text{cm}^{-1}$ 의 흡수율로 확인하였다. EVA에 나노입자가 도입됨에 따라 물성저하가 일어나는지 조사하기 위해 광 투과도와 보온성에서 우수한 특성을 보인 나노크기의  $\text{SiO}_2$ 를 함유한 필름과 마이크로 크기의  $\text{SiO}_2$ 를 함유한 필름의 인장강도, 신율, 인열강도 및 탁도를 측정하였다. 나노입자가 2 wt%의 낮은 중량비로 혼합되었기에 EVA 고유의 물성에는 크게 저하를 일으키지 않았고 오히려 인장강도 및 신율에서 물성이 증가되었다. 인열강도 및 탁도에서는 물성저하가 일어 났으나 미비한 정도였고 보온필름의 품질규격 수치를 증가하는 값이었다.

## Table of contents

Abstract (Part I) .....	i
Abstract (Part II) .....	ii
List of Figures (Part I) .....	vi
List of Figures (Part II) .....	vii
List of Tables .....	vii
Background .....	1
A brief introduction of SiO <sub>2</sub> materials .....	2
1. Chemical Formula .....	2
2. Application .....	3
3. Properties .....	3
4. Synthetic Silica .....	3
4-1. Hydrolysis.....	4
4-2. Condensation .....	4
5. Applications .....	6
5-1. Applications to Paint .....	6
5-2. Applications to Plastic Film .....	7
5-3. Applications to Beer & Beverage .....	8
5-4. Applications to Tooth Paste .....	8
 PART I .....	 9
Abstract .....	9
1. Introduction .....	10
2. Experiments .....	10
2.1. Materials and Analytical Methods .....	10
2.2. Syntheses of monodispersed nanosized-SiO <sub>2</sub> nanoparticles .....	11
2.2.1. Synthesis of SiO <sub>2</sub> nanoparticles from TEOS .....	11
2.2.2. Synthesis of aggregated microsized-SiO <sub>2</sub> nanoparticles from sodium metasilicate (Na <sub>2</sub> O · SiO <sub>2</sub> · 9H <sub>2</sub> O) .....	12
2.2.3. Synthesis of monodispersed microsized-SiO <sub>2</sub> nanoparticles from sodium silicate (Na <sub>2</sub> O · 3SiO <sub>2</sub> · xH <sub>2</sub> O) by emulsion route .....	13

2.3. Surface modification of SiO <sub>2</sub> nanoparticles .....	14
2.4. Preparation of EVA/SiO <sub>2</sub> -oleate nanocomposite and EVA/SiO <sub>2</sub> -MPS nanocomposite by inserting surface modified-SiO <sub>2</sub> nanoparticles into EVA .....	15
2.5. Pretreatments of EVA/SiO <sub>2</sub> nanocomposite for mechanical property test .....	15
3. Results and discussion .....	16
3.1. Synthesis of SiO <sub>2</sub> nanoparticles .....	16
3.2. Surface modification of SiO <sub>2</sub> nanoparticles .....	19
3.3. Dispersibility of EVA/SiO <sub>2</sub> -oleate and EVA/SiO <sub>2</sub> -MPS nanocomposite .....	22
3.4. Mechanical property test of EVA/SiO <sub>2</sub> -MPS nanocomposite .....	25
3.4.1. Selection of raw EVA .....	25
3.4.2. Abrasion resistance test of EVA/SiO <sub>2</sub> -MPS nanocomposite .....	25
3.4.3. Hardness test of EVA/SiO <sub>2</sub> -MPS nanocomposite .....	26
3.4.4. Tensile strength and elongation measurement of EVA/SiO <sub>2</sub> -MPS nanocomposite .....	27
3.4.5. The most distinguished EVA/SiO <sub>2</sub> -MPS nanocomposite .....	29
4. Summary .....	30
5. References .....	31
6. Korean abstract .....	33
 PART II .....	 34
Abstract .....	34
1. Introduction .....	35
2. Experiments .....	36
2.1. Materials and Analytical Methods .....	36
2.2. Syntheses of heat insulating nanoparticles .....	36
2.2.1. Synthesis of nanosized-SiO <sub>2</sub> nanoparticles by emulsion method .....	36
2.2.2. Synthesis of aggregated microsized-SiO <sub>2</sub> nanoparticles .....	37
2.2.3. Synthesis of Al <sub>2</sub> O <sub>3</sub> nanoparticles .....	38
2.2.4. Synthesis of MgO and CaO nanoparticles .....	38
2.3. Surface modification of heat insulating nanoparticles .....	39
2.4. Preparation of EVA/heat insulating nanocomposite and greenhouse film with heat insulating ability by inserting surface modified-nanoparticles into EVA .....	39

3. Results and discussion .....	40
3.1. Nanosized-SiO <sub>2</sub> nanoparticles .....	40
3.2. Al <sub>2</sub> O <sub>3</sub> nanoparticles .....	41
3.3. MgO nanoparticles .....	42
3.4. CaO nanoparticles .....	43
3.5. Measurement of heat insulating property of surface modified-nanoparticles .....	44
3.6. EVA/nanoparticles vinyl film with 60 $\mu$ m thickness .....	45
3.6.1. Dispersibility of surface modified-nanoparticles in EVA .....	45
3.6.2. light transparency of EVA/nanoparticles vinyl film .....	47
3.6.3. Measurement of heat insulating property of EVA/nanoparticles vinyl film .....	48
3.4. Mechanical property test for EVA/nanoparticles vinyl film .....	49
4. Summary .....	51
5. References .....	53
6. Korean abstract .....	55

## List of Figures (Part I)

Figure 1-1. Schematic drawing of the synthetic process of monodispersed nanosized-SiO<sub>2</sub> nanoparticles

Figure 1-2. Schematic drawing of the synthetic process of aggregated microsized-SiO<sub>2</sub> nanoparticles

Figure 1-3. Schematic drawing of the synthetic process of monodispersed microsized-SiO<sub>2</sub> nanoparticles

Figure 1-4. X-ray diffractograms of the SiO<sub>2</sub> powers prepared by heat treated at (a) 800 °C, (b) 1000 °C and (c) 1200 °C

Figure 1-5. SEM images of SiO<sub>2</sub> nanoparticles from (a) TEOS, (b) sodium metasilicate and (c) sodium metasilicate by emulsion method

Figure 1-6. FT-IR spectra of (a) oleic acid, (b) SiO<sub>2</sub>-oleate and (c) SiO<sub>2</sub>

Figure 1-7. TEM images of (a) SiO<sub>2</sub> nanoparticles from TEOS and (b) SiO<sub>2</sub>-oleate nanoparticle complex

Figure 1-8. FT-IR spectra of (a) MPS coated-SiO<sub>2</sub> nanoparticles and (b) uncoated-SiO<sub>2</sub> nanoparticles

Figure 1-9. SEM images of (a) SiO<sub>2</sub> nanoparticles from sodium metasilicate and (b) MPS coated-SiO<sub>2</sub> nanoparticles

Figure 1-10. Photograph images of (a) EVA, (b) EVA/SiO<sub>2</sub>-oleate-T-3, (c) EVA/SiO<sub>2</sub>-oleate-T-5 and (d) EVA/SiO<sub>2</sub>-oleate-T-10

Figure 1-11. Photograph images of EVA/SiO<sub>2</sub>-MPS nanocomposites (a) EVA/SiO<sub>2</sub>-MPS-T-3, (b) EVA/SiO<sub>2</sub>-MPS-T-5 and (c) EVA/SiO<sub>2</sub>-MPS-T-10

Figure 1-12. Photograph images of (a) EVA/SiO<sub>2</sub>-oleate-T-3 and (b) EVA/SiO<sub>2</sub>-MPS-T-3

Figure 1-13. Abrasion resistance data of EVA12/SiO<sub>2</sub>-T-3 (■) and EVA18/SiO<sub>2</sub>-T-3 (□)

Figure 1-14. Abrasion resistance data of EVA18 (▤) and EVA18/SiO<sub>2</sub>-T-3 (■), -T-5 (□), -T-10 (▨) and EVA18/SiO<sub>2</sub>-M-3 (▩), -M-5 (□), -M-10 (▨) and EVA18/SiO<sub>2</sub>-S-3 (▩), -S-5 (□), -S-10 (▨)

Figure 1-15. Hardness data of EVA18 (▤) and EVA18/SiO<sub>2</sub>-T-3 (■), -T-5 (□), -T-10 (▨) and EVA18/SiO<sub>2</sub>-M-3 (▩), -M-5 (□), -M-10 (▨) and EVA18/SiO<sub>2</sub>-S-3 (▩), -S-5 (□), -S-10 (▨)

Figure 1-16. Tensile strength data of EVA18 (▤) and EVA18/SiO<sub>2</sub>-T-3 (■) -T-5 (□) -T-

10 ( ) and EVA18/SiO<sub>2</sub>-M-3 ( ), -M-5 ( ), -M-10 ( ) and EVA18/SiO<sub>2</sub>-S-3 ( ), -S-5 ( ), -S-10 ( )

Figure 1-17. Elongation data of EVA18 ( ) and EVA18/SiO<sub>2</sub>-T-3 ( ), -T-5 ( ), -T-10 ( ) and EVA18/SiO<sub>2</sub>-M-3 ( ), -M-5 ( ), -M-10 ( ) and EVA18/SiO<sub>2</sub>-S-3 ( ), -S-5 ( ), -S-10 ( )

## **List of Figures (Part II)**

Figure 2-1. Schematic drawing of the synthetic process of nanosized-SiO<sub>2</sub> nanoparticles

Figure 2-2. Schematic drawing of the synthetic process of Al<sub>2</sub>O<sub>3</sub> nanoparticles

Figure 2-3. Schematic drawing of the synthetic process of MgO and CaO nanoparticles

Figure 2-4. TEM image of nanosized-SiO<sub>2</sub> nanoparticles

Figure 2-5. XRD spectrum of Al<sub>2</sub>O<sub>3</sub> nanoparticles

Figure 2-6. TEM image of Al<sub>2</sub>O<sub>3</sub> nanoparticles

Figure 2-7. XRD spectrum of MgO nanoparticles

Figure 2-8. TEM image of MgO nanoparticles

Figure 2-9. XRD spectrum of CaO nanoparticles

Figure 2-10. TEM image of CaO nanoparticles

Figure 2-11. FT-IR spectra of heat insulating nanoparticles

Figure 2-12. Optical microscope image of (a) EVA film, (b) EVA/Al<sub>2</sub>O<sub>3</sub>-MPS film, (c) EVA/CaO-MPS film, (d) EVA/MgO-MPS film, (e) EVA/SiO<sub>2</sub>-MPS(nano) film, (f) EVA/SiO<sub>2</sub>-MPS(micro) film

Figure 2-13. UV-vis spectra of EVA/nanoparticles film

Figure 2-14. FT-IR spectra of EVA/nanoparticles film

## **List of Tables**

Table 2-1. Mechanical property test for EVA/nanoparticles film

Table 2-2. Quality standards for heat insulating film

# Background

Worldwide studies on ceramics, polymers and metals during the last century have resulted in the establishment of materials science as a scientific discipline. A feature of these studies, particularly for ceramics, is their interdisciplinary nature and at the present time chemistry is making an increasingly important contribution to the research development and manufacture of ceramic. The main roles of chemistry we are interested are the synthesis of ceramic materials in the form of powders, coatings, fibers and monoliths. In the synthesis of these materials, several methods have been applied including conventional synthesis, co-precipitation, sol-gel process, hydrothermal method, and pyrolysis.

Silicon is the most abundant element in the earth's crust, and evidence of silicate hydrolysis and condensation to form polysilicate gels and particles is seen in many natural systems. The first metal alkoxide,  $\text{SiO}_2$ , was prepared from  $\text{SiCl}_4$  and alcohol by Ebelmen, who found that the compound gelled on exposure to the atmosphere. However, these materials remained of interest only to chemists for almost a century. It was finally recognized by Geffcken in the 1930s that alkoxides could be used in the preparation of oxide films. This process was developed by the Schott glass company in Germany and was quite well understood, as explained in the excellent review by Schoeder.

Inorganic gels from aqueous salts have been studied for a long time. Graham showed that the water in silica gel could be exchanged for organic solvents, which argued in favor of the theory that the gel consisted of a solid network with continuous porosity. Competing theories of gel structure regarded the gel as a coagulated sol with each of the particles surrounded by a layer of bound water, or as an emulsion. The network structure of silica gels was widely accepted in the 1930s, largely through the work of Hurd, who showed that they must consist of a polymeric skeleton of silicic acid enclosing a continuous liquid phase. The process of supercritical drying to produce aerogels was invented by Kistler in 1932, who was interested in demonstrating the existence of the solid skeleton of the gel, and in studying its structure. Around the same time, mineralogists became interested in the use of sols and gels for the preparation of homogeneous powders for use in studies of phase equilibrium. This method was later

popularized in the ceramics community by Roy for the preparation of homogeneous powders. That work, however, was not directed toward an understanding of the mechanisms of reaction or gelation, nor the preparation of shapes (monoliths). Much more sophisticated work, both scientifically and technologically, was going on in the nuclear fuel industry, but it was not published until later. The goal was to prepare small spheres of radioactive oxides that would be packed into fuel cells for nuclear reactors. The advantage of sol-gel processing was that it avoided generation of dangerous dust, as would be produced in conventional ceramics processing, and facilitated the formation of spheres. The latter was accomplished by dispersing the aqueous sol in a hydrophobic organic liquid, so that the sol would form into small droplets, each of which would subsequently gel. The ceramics industry began to show interest in gels in the late sixties and early seventies. Controlled hydrolysis and condensation of alkoxides for preparation of multicomponent glasses was independently developed by organometallic precursors on a commercial basis by several companies. However, the explosion of activity that continues today can be dated from the demonstration by Yoldas and Yamane et al. that monoliths could be produced by careful drying of gels. This is a bit ironic in retrospect, as it is evident that monoliths are the least technologically important of the potential applications of gels. However, the allure of a room-temperature process for the preparation of bricks and windows was irresistible for research directors around the world, and enormous effort has been devoted to demonstrating that the objective is nonsense. As it is usually the case, the technology preceded the science of sol- gel processing, but great strides have been made in the past few years in understanding the fundamental aspects of preparing homogeneous multicomponent ceramics (crystalline and amorphous) from alkoxide derived gels.

## A brief introduction of SiO<sub>2</sub> materials

### 1. Chemical Formula

: SiO<sub>2</sub> (Silica)

## 2. Application

- Matting agent for paint (wood/industrial/PCM) and ink
- Antiblocking agent for plastic film (PP, PE, PET etc.)
- Printability improving agent for inkjet paper, film or textile
- Antifoaming aids
- Anti-caking agent for deliquescent powder
- Stabilizer for beer
- Abrasive for transparent toothpaste
- Solid carrier

## 3. Properties

The physicochemical properties of concern with the silica are the porosity (represented by the specific surface area, pore volume, pore-size distribution and bulk density), surface coverage of the silanol groups and water molecules (indicated by the ignition loss, moisture content, pH, impurity level and surface curvature), as well as the size of particles (i.e. mean size and size distribution). In practical applications, however, most of these properties do work together and therefore the properties of the synthetic nanosized silica compatible with a specific application depend necessarily on the characteristics of the application system. Various grades of the nanosized or micro-sized silica are offered for this reason.

The porosity of the nanosized or micro-sized silica is determined largely in the course of the aging process, and surface coverage of silanol groups finally at the washing, drying and/or surface-treatment step, and the control of particle size is up to the milling section.

## 4. Synthetic Silica

Silica (i.e. silicon dioxide:  $\text{SiO}_2$ ) is most plentiful natural resources on the earth, and is a tasteless, odorless and harmless solid. The synthetic silica, distinguished from the naturally occurring silica, is artificially made in order to give a specific property and purity to it, and the synthetic silica is generally amorphous whereas the natural silica is

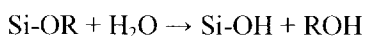
mostly crystalline.

The synthetic silica is widely used as absorbent, abrasive, catalyst support, thickening agent, free-flowing aid, anti blocking agent, matting agent and so forth.

The synthetic silica which has pores in it, is made from water glass through the reaction with a mineral acid. The synthetic silica may be used for the whole field of silica applications and is composed of what is called the primary particle whose size is on nanometers order. These primary particles look like nonporous spheres and inside them many three-dimensional networks of siloxane microstructure exist, and they get agglomerated and interconnected by a number of siloxane bridges to form network structures of particulates and thereby many tunnels of pores in-between.

#### **4-1. Hydrolysis**

Hydrolysis occurs by the nucleophilic attack of the oxygen contained in water on the silicon atom as evidenced by the reaction of isotopically labeled water with TEOS that produces only unlabelled alcohol in both acid- and base- catalyzed systems:



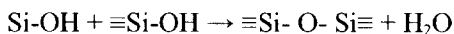
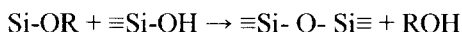
The same behavior is observed in organo-alkoxysilanes,  $\text{R}_x\text{Si(OR)}_{4-x}$ , where  $x = 1, 2$ , or  $3$ .

Tetraalkoxysilanes, organotrialkoxysilanes, and diorganodialkoxysilanes hydrolyse upon exposure to water vapor. Hydrolysis is facilitated in the presence of homogenizing agents (alcohols, dioxane, THF, acetone, etc.) that are especially beneficial in promoting the hydrolysis of silanes containing bulky organic or alkoxy ligands, such as phenylphenoxysilane, which, when neat (undiluted), remains unhydrolyzed upon exposure to water vapor. It should be emphasized, however, that the addition of solvents may promote esterification or depolymerization reactions. Control of the hydrolysis rate should be considered with those following factors; effect of catalysts, steric and inductive effects, reactant ratio, and solvent effect.

#### **4-2. Condensation**

Polymerization to form siloxane bonds occurs by either an alcohol producing condensation or a water-producing condensation reaction. The latter reaction has been

discussed in detail by Iler with regard to forming silicate polymers and gels in aqueous media.



Engelhardt and coworkers employed  $^{29}\text{Si}$  NMR to investigate the condensation of aqueous silicates at high pH. Their results indicate that typical sequence of condensation products are monomer, dimer, linear trimer, cyclic trimer, cyclic tetramer, and higher-order rings. The rings form the basic framework for the generation of discrete colloidal particles commonly observed in aqueous systems.

This sequence of condensation requires both depolymerization and the availability of monomers, which are in solution equilibrium with the oligomeric species and/or are generated by depolymerization. However in alcohol - water solutions normally employed in sol - gel processing, the depolymerization rate is lower than in aqueous media, especially at low pH. Control of the condensation rate should be considered with those following factors; effect of catalysts, steric and inductive effects, and solvent effect.

- Sol:

➔ A solution of various reactants that are undergoing hydrolysis and condensation reactions. The molecular weight of the oxide species produced continuously increases. As these species grow, they may begin to link together in a three-dimensional network.

- Gel Point:

➔ The point in time at which the network of linked oxide particles spans the container holding the sol. At the gel point the sol becomes an alcogel.

- Alcogel (wet gel):

➔ At the gel point, the mixture forms a rigid substance called an alcogel. The alcogel can be removed from its original container and can stand on its own. An alcogel consists of two parts, a solid part and a liquid part. The solid part is formed by the three-dimensional network of linked oxide particles. The liquid part (the original solvent of the sol) fills the free space surrounding the solid part. The liquid and solid parts of an alcogel

occupy the same apparent volume.

- **Supercritical fluid:**

→ A substance that is above its critical pressure and critical temperature. A supercritical fluid possesses some properties in common with liquids (density, thermal conductivity) and some in common with gases (fills its container, does not have surface tension).

- **Aerogel:**

→ What remains when the liquid part of an alcogel is removed without damaging the solid part (most often achieved by supercritical extraction). If made correctly, the aerogel retains the original shape of the alcogel and at least 50% (typically >85%) of the alcogel's volume.

- **Xerogel:**

→ What remains when the liquid part of an alcogel is removed by evaporation, or similar methods. Xerogels may retain their original shape, but often crack. The shrinkage during drying is often extreme (~90%) for xerogels.

## **5. Applications**

### **5-1. Applications to paint**

#### **→ High-tech on the edge of brush**

The nanosized or micro-sized silica as a matting or thickening agent applies to a variety of paints such as lacquer, polyurethane, epoxy, alkyd, hydrolic and metallic paints etc. and these paints matted by silica are normally used for the household furniture exhibiting an antique decoration as well as for the industrial purpose of mainly metals pre-coating where a glossy environment is undesirable. The nanosized or micronized silica added in a paint is floating toward the surface of the paint film and thus makes the film surface rough in a microscopic sense. This rough surface induces a diffused reflection of incident rays, which gives the matting effect on the paint. In addition, the silica increases more or less both the viscosity and the thixotropy of the paint which facilitates painting. The silica

makes no adverse effect on paint itself in the respect of the paint-segment flow-ability and hardening, the paint recoating, the paint-film transparency and stiffness, the paint-film resistance to corrosion and erosion, and so forth. As to the transparency and stiffness of the paint film, the compatibility between the silica and base polymer resin is crucial as illustrated in the section of applications to plastic film. The surface of the silica particles is covered partly with silanol groups (i.e.-OH) which render the silica surface somewhat hydrophilic. In some organic-phase systems, the hydrophilicity may cause such critical problems, masking (or coating) of the silica surface with a third material, say a sort of wax, is sometimes necessary.

## **5-2. Applications to Plastic Film**

### **→Glossy world & transparent plastics**

The nanosized or micronized silica as an anti-blocking and/or slip agent is commonly applied to a number of plastic films, such as polypropylene film, polyethylene film, PET film, polyvinylchloride film etc., where the anti-blocking effect is required without any signification loss of transparency. The refractive index of the nanosized or micro-sized silica is nearly the same as those of the polymer resin, so that the plastic film can maintain its transparency.

A careful attention should be paid to the selection of a proper grade of the nanosized or micro-sized silica, in that such effects appearing as slippage, anti-blocking, transparency and stiffness vary with the compatibility between the polymer resin and the silica. In other words, to acquire all of the desired properties of a plastic film, one should cautiously take into account the physicochemical property interaction occurring between the silica and the polymer resin. For instance, as to the polypropylene film, an experience indicates that the propylene resin produced under the more active catalytic condition prefers the less porous silica. In general, the property of polymer resin associated largely with the silica property (i.e. the porosity, the surface coverage of silanol groups and water molecules and the particle size) is presumed to be the polymer structure and polymer-melt behavior as well, that is, the average molecular weight and MW (weight average molecular weight) distribution (i.e. polymer-chain length), the polymer-chain entanglement and the crystallinity etc.

### **5-3. Applications to beer & beverage**

#### **→ Smart taste & appearance**

Beer is a typical alcoholic beverage containing a lot of protein when brewed and, due to presence of the protein followed by coalescence of the protein molecules, the beer tends to get spoiled in taste and cloudy in appearance. These phenomena are often encountered, particularly when the beer undergoes a long-term storage or even moderate temperature rise. To prevent this, the undesirable portion of the protein should be eliminated in part from the beer, without loss of original taste, by treating it with excellent filterability aided by diatomaceous earth and with neither dusting nor suspension problem.

For the nanosized or micro-sized silica to suspend well in such an aqueous liquid, to adsorb selectively the protein having a certain length of molecular chain and not to cause dusting, comparatively large size of hydrophilic silica particles with a specific range of pore sizes should be made through an additional treatment.

### **5-4. Applications to Tooth Paste**

#### **→ White & bright teeth breathing fresh air**

The nanosized or micro-sized silica also has a refined function of abrasion, and it is not uncommon in advanced countries that the silica is widely used as an abrasive filler, on behalf of fumed silica (or of white carbon), to formulate either transparent or opaque toothpaste. The abrasive function of the silica relies largely on both the particle size and porosity.

## **PART I**

### **Preparation of MPS (mercaptopropyl trimethoxysilane) Coated-SiO<sub>2</sub> Nanoparticles and Effect on Mechanical Properties of EVA/SiO<sub>2</sub> Nanocomposite**

**Sung Woo Kim**

Research Advisor : Prof. Young Soo Kang

*Department of Chemistry, Graduate School, Pukyong National University*

#### **Abstract**

SiO<sub>2</sub> nanoparticles were synthesized from different three precursors such as TEOS (tetraethyl orthosilicate), sodium metasilicate and sodium silicate. First, SiO<sub>2</sub> nanoparticles were prepared by a controlled hydrolysis of TEOS. In other method, by precipitation in an emulsion medium from sodium metasilicate and hydrochloric acid solution, SiO<sub>2</sub> nanoparticles were prepared. At last, SiO<sub>2</sub> nanoparticles were also synthesized from sodium silicate by emulsion method.

In this study, we concentrated on dispersion and compatibility between nanosized SiO<sub>2</sub> particles and EVA (ethylene vinylacetate). Therefore surface modification of synthesized SiO<sub>2</sub> nanoparticles was accomplished with MPS (3-mercaptopropyl trimethoxysilane) to enhance homogeneous dispersion and compatibility between obtained SiO<sub>2</sub> nanoparticles and EVA. Finally, nanocomposites of surface treated SiO<sub>2</sub> nanoparticles and EVA were prepared. By inserting the MPS coated-SiO<sub>2</sub> nanoparticles into EVA, abrasion resistance and hardness were increased remarkably. On the other hand, insertion of SiO<sub>2</sub> nanoparticles barely decreased original tensile strength and elongation of EVA. Consequently, MPS coated-SiO<sub>2</sub>/EVA nanocomposite can have an improved abrasion resistance and hardness compared with raw EVA, without decrease tensile strength and elongation.

The characterization of synthesized SiO<sub>2</sub> nanoparticles and their nanocomposite with EVA was conducted by TEM, SEM, FT-IR, photographs and mechanical property test such as abrasion, hardness, tensile strength and elongation.

## **1. Introduction**

Precipitated silica is widely used in many consumer products. The numerous applications vary from fillers for rubber tires to additives in toothpaste. SiO<sub>2</sub> nanoparticles are white-colored powder which has characteristic of low density and high surface area. When SiO<sub>2</sub> nanoparticles were inserted into matrix such as plastic and rubber, it increases abrasion resistance, hardness and heat resistance. SiO<sub>2</sub> nanoparticles are commercially used as additives for plastic, rubber and paints. Because EVA is lack of abrasion resistance, hardness and slip property so by inserting SiO<sub>2</sub> nanoparticles into EVA, EVA can have an increased abrasion resistance, hardness and environmental affinity. For this reason, this work is mainly aimed at preparation of MPS coated-SiO<sub>2</sub>/EVA nanocomposite which will be applied to SiO<sub>2</sub>/EVA nanocomposite. SiO<sub>2</sub> nanoparticles were synthesized from TEOS, sodium metasilicate and sodium silicate by emulsion method. We also needed to conduct surface modification of SiO<sub>2</sub> nanoparticles to enhance stability in atmosphere and compatibility between EVA and SiO<sub>2</sub> nanoparticles. Surface modification was done by oleic acid and MPS. Those are optimized for the best physical properties at process ability, abrasion resistance and hardness.

## **2. Experiments**

### **2.1. Materials and analytical methods**

Tetraethylorthosilicate (C<sub>8</sub>H<sub>20</sub>O<sub>4</sub>Si, 98%, Aldrich), ammonia solution (NH<sub>4</sub>OH, Junsei), hydrochloric acid (HCl, Aldrich), sodium metasilicate (Na<sub>2</sub>O · SiO<sub>2</sub> · 9H<sub>2</sub>O, Aldrich), oleic acid (C<sub>17</sub>H<sub>33</sub>COOH, Junsei) and MPS (C<sub>6</sub>H<sub>16</sub>O<sub>3</sub>SSi, Aldrich) and EVA(ethylene vinylacetate), EF-443 from Hyundai Petrochemical Co. were used in their commercial form. Transmission electron microscopy (TEM) images were obtained by using a HITACHI, H-7500.

Scanning electron microscopy (SEM) images were obtained with HITACHI S-2400. X-ray powder diffraction (XRD) was obtained with a Philips, X'Pert-MPD system. Fourier Transform Infrared Spectroscopy (FT-IR) spectrum was obtained by using PERKIN ELMER SPECTRUM 2000. The tensile strength and elongation were measured with SHIMADZU, AG-10TG according to KSM 6518. Abrasion resistance was tested with Daekyong Tech, DTA-410 according to KSM 6625. Hardness was measured with Akashi Corp., HH-315 according to KSM 6518.

## 2.2. Syntheses of monodispersed nanosized-SiO<sub>2</sub> nanoparticles

### 2.2.1. Synthesis of SiO<sub>2</sub> nanoparticles from TEOS

We synthesized monodispersed and spherical SiO<sub>2</sub> nanoparticles by the hydrolysis of tetraethylorthosilicate (TEOS) in aqueous ethanol solution containing ammonia<sup>1</sup>. Ammonium hydroxide and deionized water were mixed in ethanol at the molar ratio of 0.5 M with stirring for 30 min. After 30 min, TEOS was added into the solution at the molar ratio of 0.2 M. The solution was stirred at room temperature for 12 hrs. As condensation reactions progress the sol will set into a rigid gel. At this point, the gel is usually removed from its mold. However, the gel must be kept covered by alcohol to prevent evaporation of the liquid contained in the pores of the gel. Evaporation causes severe damage to the gel and will lead to poor quality aerogels. For this reason, the reactant should be recovered by centrifugation. After aging the gel, all water still contained within its pores must be removed prior to drying. This is simply accomplished by soaking the gel in pure alcohol several times until all the water is removed. The obtained powder was washed six times with 30 ml of pure ethanol by repeated centrifugation and ultrasonic dispersion cycle in order to remove water within gel and impurities, such as ammonia, water, and unreacted tetraethylorthosilicate. Finally monodispersed and spherical SiO<sub>2</sub> nanoparticles were obtained.

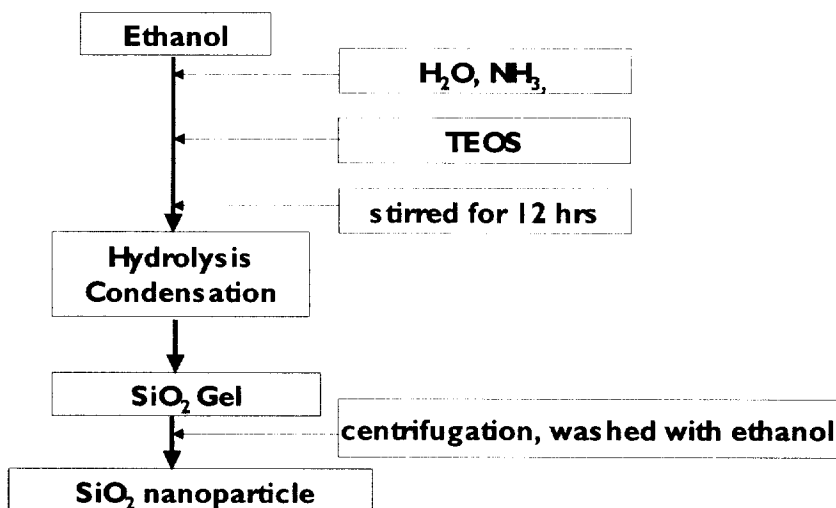


**Fig. 1-1 Schematic drawing of the synthetic process of monodispersed nanosized-SiO<sub>2</sub> nanoparticles**

### 2.2.2. Synthesis of aggregated microsized-SiO<sub>2</sub> nanoparticles from sodium metasilicate (Na<sub>2</sub>O · SiO<sub>2</sub> · 9H<sub>2</sub>O)

We synthesized SiO<sub>2</sub> nanoparticles from sodium metasilicate by relatively simple method<sup>2, 3</sup>. The precipitation of silica is achieved by the reaction of hydrochloric acid and sodium silicate. The process is performed at high pH for a definite period of time. The sol-gel process which eventually leads to a particle suspension in water can be divided in three stages. During the first stage added monomer condenses to form larger compounds. These polymeric clusters are initially stabilized by solvation. However, as they grow in size and become more compact they are finally separated from solution. Thus a solid particle is generated. This initial stage can be referred to as a growth process. The simultaneous addition of sodium ions leads to a change of the particle interaction forces. At high pH values almost all silanol groups on a silicon dioxide particle are charged negatively. However the screening effect of the positive sodium ions result in the initiation of an aggregation process. The exact conditions under which particles join to form aggregates are influenced by the size of the particle and the

magnitude of the critical coagulation concentration. During this second aggregation stage particles form colloidal fractal structures. As the concentration of particles is raised the colloidal solution becomes more viscous. The third stage of the process involves the destruction of the gel by mechanical force. The reactants were continuously added for 90 mins at pH values between 8 and 10. The mol ratio of  $\text{SiO}_2$  to  $\text{Na}_2\text{O}$  in sodium silicate solution was 3.3. The mass fraction of these two components in solution was 38%. Since the condensation reaction between monomers and silanol groups is triggered by the presence of protons, any type of acid can be used for this process. Hydrochloric acid was selected and diluted to 50 mass% HCl. Usually the sodium silicate flow was set to a constant value whereas the addition of hydrochloric acid was adjusted to maintain a constant pH.

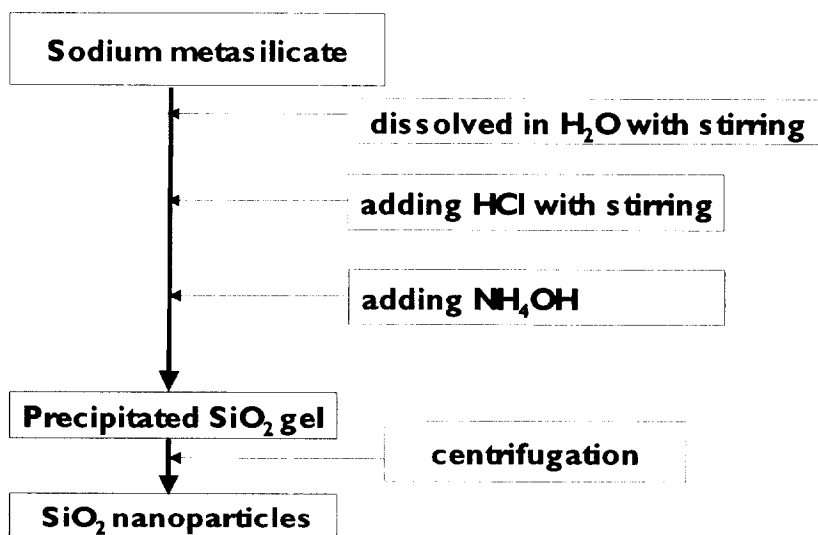


**Fig. 1-2 Schematic drawing of the synthetic process of aggregated microsized-SiO<sub>2</sub> nanoparticles**

2.2.3. Synthesis of monodispersed microsized-SiO<sub>2</sub> nanoparticles from sodium silicate ( $\text{Na}_2\text{O} \cdot 3\text{SiO}_2 \cdot \text{XH}_2\text{O}$ ) by emulsion route

Sodium silicate and ionized water were mixed at the volume ratio of 1 : 1. Span

80, emulsifier, was dissolved in kerosene at the volume ratio of 1%. And then sodium silicate solution and emulsifier solution were mixed at the ratio of 1 : 3. This solution was put into homomixer and stirred at 10,000 rpm for 60 min.  $\text{NH}_4\text{HCO}_3$ , ethanol and water were added into homomixer. The solvents were evaporated and dried at 100 °C for 24 hrs. Finally  $\text{SiO}_2$  nanoparticles were obtained<sup>4,5</sup>.

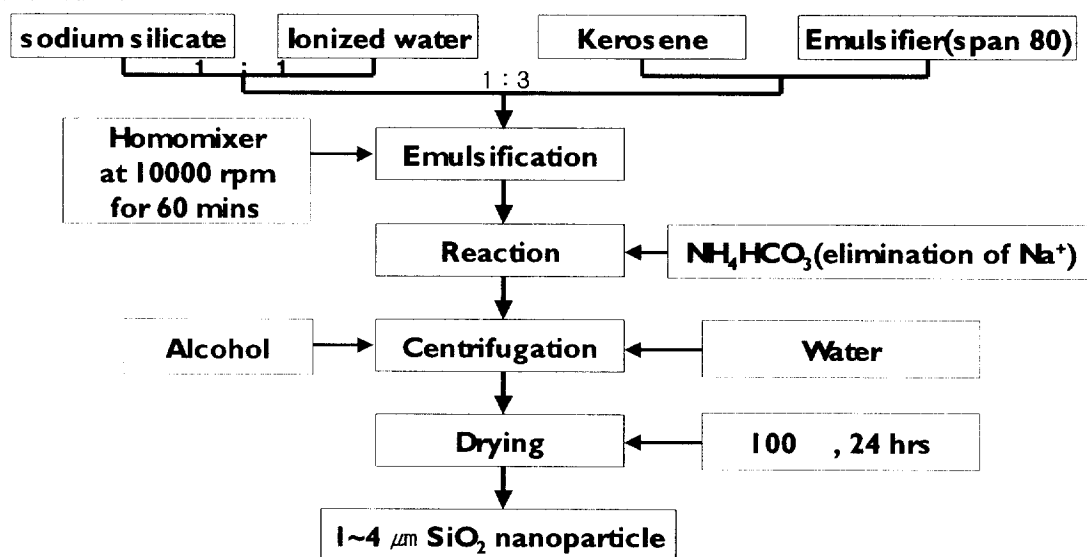


Fig. 1-3 Schematic drawing of the synthetic process of monodispersed microsized-SiO<sub>2</sub> nanoparticles from sodium silicate

### 2.3. Surface modification of SiO<sub>2</sub> nanoparticles

Surface modification of the obtained SiO<sub>2</sub> nanoparticles from TEOS was done by oleic acid. And the obtained SiO<sub>2</sub> nanoparticles can also be coated with MPS to enhance dispersive property and stability of SiO<sub>2</sub> surface in the polymer matrices. The synthesized SiO<sub>2</sub> nanoparticles were kept in 0.1 M HCl overnight. Ammonium hydroxide and deionized water were mixed in ethanol at the molar ratio of 0.5 M and either oleic acid or MPS was dissolved in ethanol with stirring. After the silane coupling agents were hydrolyzed for 1 hr, silica (pretreated with HCl) was added. The solution was put into autoclavable bottle and heated to

300 °C for 6 hrs. After 6 hrs, solvent was evaporated, washed with ethanol and dried at room temperature. Finally, SiO<sub>2</sub>-oleate and MPS coated-SiO<sub>2</sub> complexes were obtained.

#### 2.4. Preparation of EVA/SiO<sub>2</sub>-oleate nanocomposite and EVA/SiO<sub>2</sub>-MPS nanocomposite by inserting surface modified-SiO<sub>2</sub> nanoparticles into EVA

The obtained SiO<sub>2</sub>-oleate nanoparticles and MPS coated-SiO<sub>2</sub> nanoparticles were separately used at the ratio of 3 wt%, 5 wt% and 10 wt%. EVA contents were fixed at 10 g. EVA was well swelled in xylene at 80 °C. SiO<sub>2</sub> nanoparticles were dispersed in xylene. Then the solution of SiO<sub>2</sub> nanoparticles was added into solution of containing EVA with stirring at 80 °C for 1 hr. After 1 hr, the solution was kept at 40 °C for 12 hrs. Remaining xylene was completely eliminated in vacuum oven at 50 °C for 2 days. Finally, EVA/SiO<sub>2</sub>-oleate and EVA/SiO<sub>2</sub>-MPS nanocomposite were obtained.

#### 2.5. Pretreatments of EVA/SiO<sub>2</sub> nanocomposite for mechanical property test

The obtained EVA/SiO<sub>2</sub>-MPS nanocomposites were compressed into 0.2 mm thickness sheet by using hot-press at 120 °C for 5 mins. To do the test of abrasion resistance, EVA/SiO<sub>2</sub>-MPS nanocomposite was also pretreated with hot-press according to KSM 6625. Mechanical property tests such as abrasion resistance, tensile strength, elongation and hardness of the pretreated nanocomposite were conducted.

### 3. Results and discussion

#### 3.1. Synthesis of SiO<sub>2</sub> nanoparticles

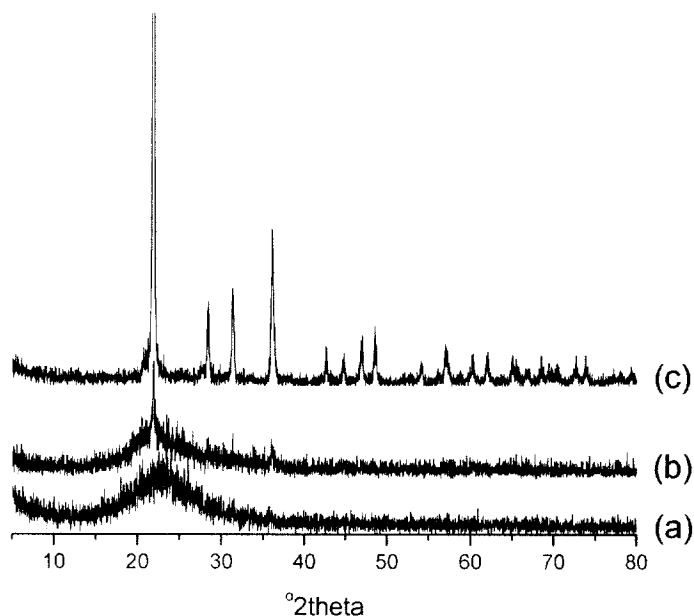


Fig. 1-4 X-ray diffractograms of the SiO<sub>2</sub> powers prepared by heat treated at (a) 800 °C, (b) 1000 °C and (c) 1200 °C

The X-ray diffraction patterns show that the precursor slowly changed to the calcined SiO<sub>2</sub> nanoparticle as increasing calcination temperature. Fig. 1-4 shows that diffraction patterns of SiO<sub>2</sub> nanoparticle corresponding to cristobalite SiO<sub>2</sub> have been found for the samples calcined at 1200 °C. No significant change in the structure has been found after heat-treatment temperature up to 1000 °C. A small amount of SiO<sub>2</sub> has been detected after calcination below 1000 °C, but most of them are assigned as an amorphous structure. The single-phase cristobalite SiO<sub>2</sub> has been observed in the sample calcined at 1200 °C for 24 hrs. Cristobalite is form of crystalline silica. Cristobalite is thermally altered forms of quartz. It may be present in areas where substances containing quartz are heated, such as in refractories, sintering, calcination, or heat expansion.

In pure alcohol solvent (usually ethanol), the final particle size mainly depended on the initial water and ammonia concentration. Zukoski et al. studied on the relationships of the final particle size and the concentrations of  $\text{NH}_3$  and  $\text{H}_2\text{O}$ . In addition, the properties of alcohol have an important effect on the hydrolysis, condensation rates and the final particle size. Sadasivan et al. and Harris et al. reported that the final particle size increased as the molecular weight of alcohol increased, and assumed that this might be due to the change of viscosity or the polarity of the solvent.

The average size of  $\text{SiO}_2$  nanoparticles from TEOS was determined as 150 nm by SEM image. The particles show spherical shape that may represent the simplest form that a colloidal particle can easily adopt during the nucleation or growth process, as driven by minimization of interfacial energy. Scanning electron microscopy (SEM) examinations of the samples were carried out on a HITACHI S-2400. All powders were dried under vacuum for 6 hrs at 100 °C before the characterization. The particles are monodispersed and spherical shape (Fig. 1-5 (a)). Fig. 1-5 (b) shows SEM image of  $\text{SiO}_2$  nanoparticles from sodium metasilicate. The precipitation process of silica can be divided into three stages. During the first stage the primary particles grow in size. The growth process is followed by an aggregation stage, where particles aggregate to form larger clusters until a viscous gel is formed. During the last stage the gel is destroyed by mechanical force and due to compaction of the clusters. Therefore particles decrease in size with time during this stage. A decrease of energy input and not enough energy input during the aggregation and destruction stages result in the formation of larger and less compact particles at the end of the precipitation process. In our experiment, especially additional energy input was not induced. For this reason, the obtained particles were large and aggregated. There is one other reason why monodispersed particles were not obtained. To achieve monodispersity, nucleation and growth stages must be strictly separated and nucleation should be avoided during the period of growth. In a closed system, the monomer (usually exists as a complex or a solid precursor) must be added or released slowly at a well-controlled rate in order to keep it from passing the

critical supersaturation levels during the growth period. In our experiment, it can be assumed that nucleation was occurred during growth so that particles tended to make agglomerations. In Fig. 1-5 (b), these particles are non-spherical, aggregated and larger than  $\text{SiO}_2$  nanoparticles from TEOS up to  $\mu\text{m}$ . Fig 1-5. (c) is SEM image of  $\text{SiO}_2$  nanoparticles from sodium silicate by emulsion route. These particles are larger than those from TEOS. But, in comparison with  $\text{SiO}_2$  nanoparticles from sodium metasilicate,  $\text{SiO}_2$  nanoparticles from sodium silicate was more homogeneous and spherical shape. The particle size is from 1  $\mu\text{m}$  to 4  $\mu\text{m}$ .

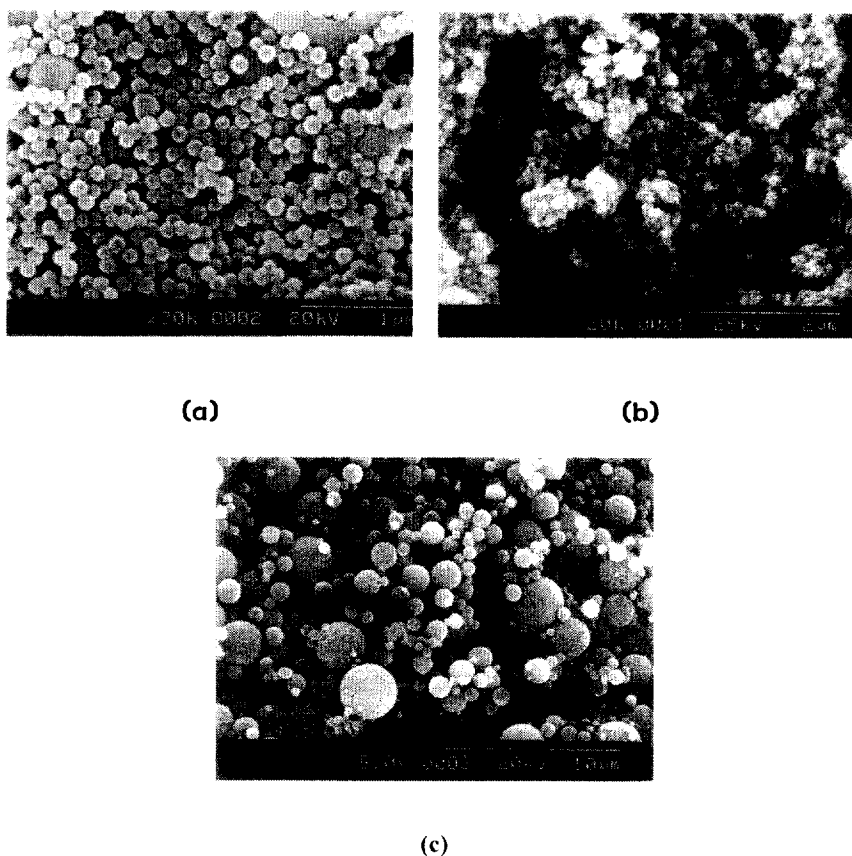


**Fig. 1-5 SEM images of  $\text{SiO}_2$  nanoparticles from (a) TEOS, (b) sodium metasilicate and (c) sodium metasilicate by emulsion method**

### 3.2. Surface modification of SiO<sub>2</sub> nanoparticles

Fig. 1-6 presents FT-IR spectra of (a) oleic acid, (b) SiO<sub>2</sub>-oleate and (c) SiO<sub>2</sub> prepared from TEOS.

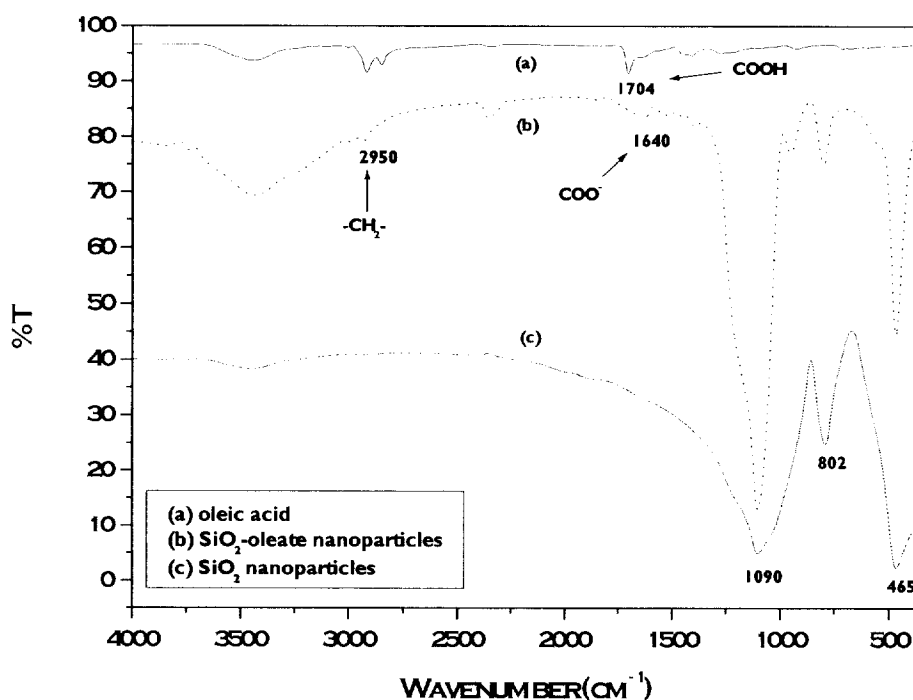


**Fig. 1-6** FT-IR spectra of (a) oleic acid, (b) SiO<sub>2</sub>-oleate and (c) SiO<sub>2</sub>

In spectrum (c), the typical peaks of Si-O were observed at 465, 802 and 1090 cm<sup>-1</sup>. The bands at 1090 and 802 cm<sup>-1</sup> are due to asymmetry stretching and symmetry stretching band of SiO<sub>4</sub><sup>-4</sup> tetrahedral structure<sup>6,7</sup>. Si-O rocking band is found at 465 cm<sup>-1</sup>. In spectrum (a), the peak of -COOH in oleic acid was confirmed at 1704 cm<sup>-1</sup>. Spectrum (b) is SiO<sub>2</sub>-oleate nanoparticles. In comparison with spectrum (c) of raw SiO<sub>2</sub> nanoparticles, spectrum (b) also includes the typical peaks of SiO<sub>2</sub> with new peak of -COO<sup>-</sup> appeared at 1640 cm<sup>-1</sup>. In addition, the bands at 2950 cm<sup>-1</sup> is attributed to the symmetric stretching of -CH<sub>2</sub>- which comes from oleic acid. So it is concluded that SiO<sub>2</sub>-oleate nanoparticles were

successfully prepared by chemical reaction between SiO<sub>2</sub> nanoparticles and oleic acid.

To compare dispersibility before surface modification and after surface modification, TEM measurement was conducted. Transmission electron microscopy (TEM) examinations of the samples were carried out on a HITACHI H-7500 transmission electron microscope. TEM samples were prepared on the 400 mesh copper grid coated with carbon. SiO<sub>2</sub> nanocrystallite monolayer was formed by self-assembly when a drop of the SiO<sub>2</sub> nanoparticle ethanol solution was carefully placed on the copper grid and dried in air. The prepared SiO<sub>2</sub>-oleate nanoparticles have an improved dispersion property compared with raw SiO<sub>2</sub> nanoparticles (Fig. 1-7).

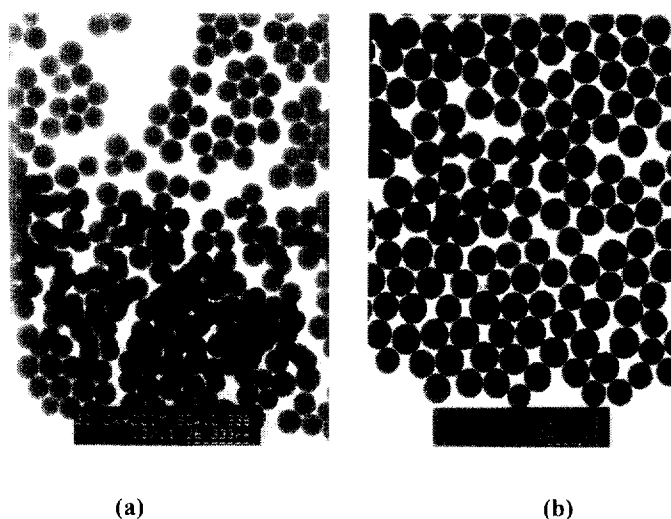


**Fig. 1-7 TEM images of (a) SiO<sub>2</sub> nanoparticles from TEOS and (b) SiO<sub>2</sub>-oleate nanoparticle**

Nowadays the silanization of the silica surface is a convenient method to modify the surface properties or to introduce functional groups to the silica support material<sup>8,9</sup>. silane coupling agents have been used in the rubber industry to improve the performance of silica and other mineral fillers in rubber compounds. A silane coupling agent contains functional groups that can react with

the rubber and the silica. Grafting of the MPS molecules is believed to take place as follows. First, the methoxy groups of MPS hydrolyze under the influence of the base and water. Silanols are formed which associate and form oligomers. These oligomers adsorb on the silica surface by hydrogen bonding and condense on drying to form siloxane linkages.

Fig. 1-8 shows coating of MPS onto silica surface. In comparison with uncoated  $\text{SiO}_2$  (Fig. 1-8 (b)), spectrum of MPS coated- $\text{SiO}_2$  (Fig. 1-8 (a)) shows new peaks which came from MPS. One peak that represents -SH appears at  $2561\text{ cm}^{-1}$  and another peak that represents asymmetric stretching vibration of  $-\text{CH}_2-$  appears at  $2930\text{ cm}^{-1}$ . So we can conclude that MPS coating onto  $\text{SiO}_2$  surface was successfully done. The prepared MPS coated- $\text{SiO}_2$  nanoparticles (Fig. 1-9 (b)) from sodium metasilicate are also well dispersed compared with raw  $\text{SiO}_2$  nanoparticles (Fig. 1-9 (a)).

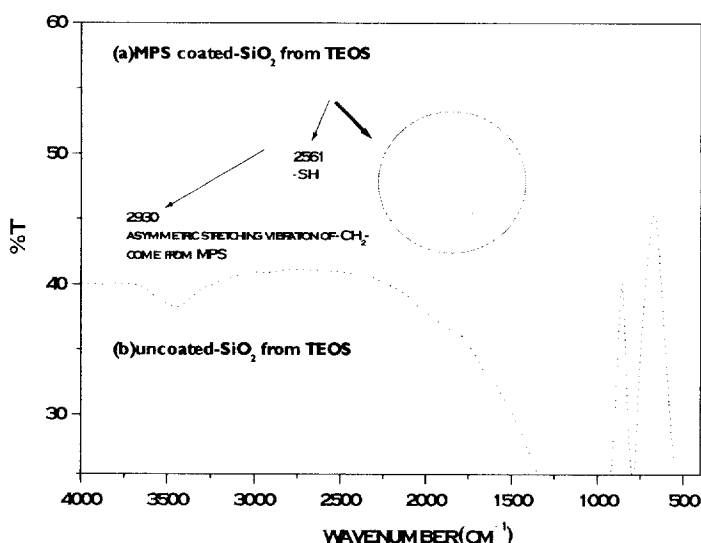
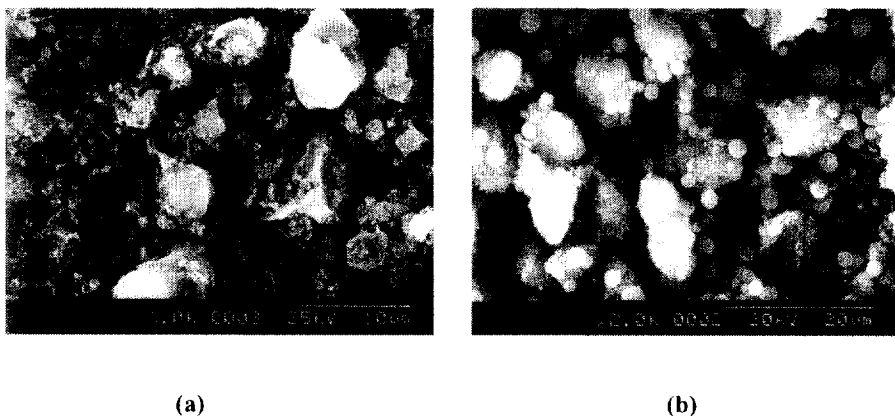


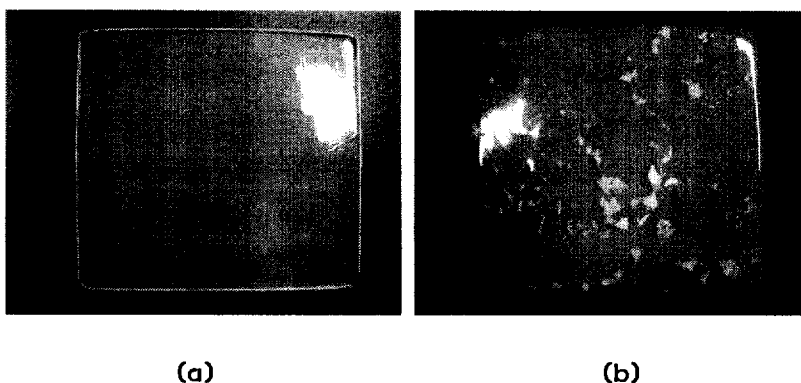
Fig. 1-8 FT-IR spectra of (a) MPS coated- $\text{SiO}_2$  nanoparticles and (b) uncoated- $\text{SiO}_2$  nanoparticles

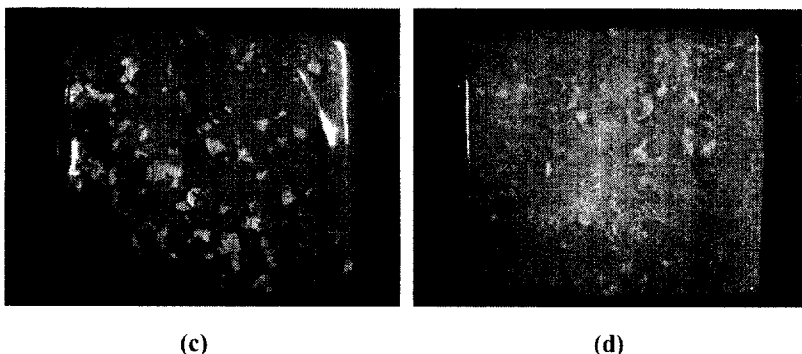


**Fig. 1-9 SEM images of (a)  $\text{SiO}_2$  nanoparticles from sodium metasilicate and (b) MPS coated- $\text{SiO}_2$  nanoparticles**

### 3.3. Dispersibility of EVA/ $\text{SiO}_2$ -oleate and EVA/ $\text{SiO}_2$ -MPS nanocomposite

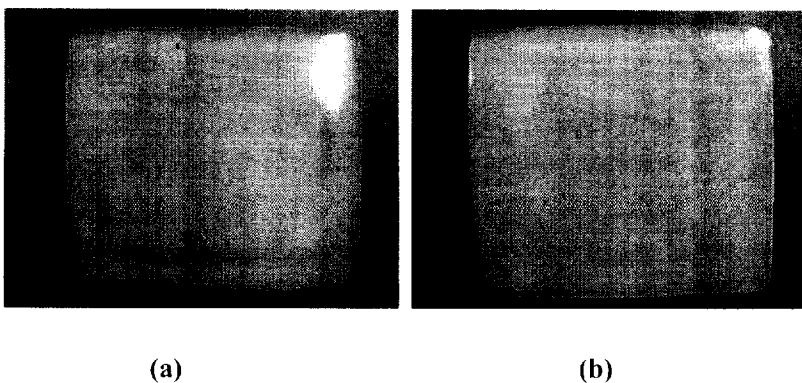
At this point of time, we need to define kinds of nanocomposite to represent them concisely. EVA means raw EVA not containing  $\text{SiO}_2$  and EVA12 and 18 means its VA (vinyl acetate) contents (%). -T-, -S- and -O- represent  $\text{SiO}_2$  synthesized from TEOS, sodium metasilicate and sodium silicate in order, respectively. 3, 5 and 10 means inserted wt% of  $\text{SiO}_2$  into EVA. Fig. 10 shows dispersibility of  $\text{SiO}_2$ -oleate into EVA. All of the EVA/ $\text{SiO}_2$ -oleate nanocomposite did not show satisfactory dispersibility and formed large agglomerations of  $\text{SiO}_2$ -oleate (Fig 1-10). Thus we can conclude that oleate coating onto  $\text{SiO}_2$  could not enhance compatibility between EVA and  $\text{SiO}_2$  but enhance stability in atmosphere.

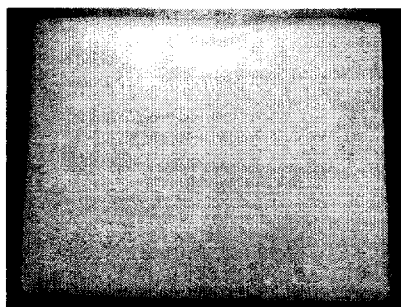




**Fig. 1-10 Photograph images of (a) EVA, (b) EVA/SiO<sub>2</sub>-oleate-T-3, (c) EVA/SiO<sub>2</sub>-oleate-T-5 and (d) EVA/SiO<sub>2</sub>-oleate-T-10**

In Fig. 1-11, we confirmed MPS coated-SiO<sub>2</sub> nanoparticles were well dispersed into EVA and rarely aggregated in all of the nanocomposite compared with EVA/SiO<sub>2</sub>-oleate nanocomposite (Fig. 1-12). The success of encapsulation was highly dependent on the nature of the silica particle surface. Thus, successful encapsulation was achieved when MPS-coated silica particles were engaged in the preparation of silica-polymer nanocomposite. Because, by grafting MPS onto silica surface, the silica particle surface is changed from hydrophilic to hydrophobic so that irreversible aggregation of the silica particles are prevented<sup>10, 11</sup>. Furthermore, induced hydrophobic groups also have functional group that can form covalent bonds between silica and polymer. On the contrary, encapsulation of the MPS unmodified-silica particles failed to occur (Fig. 1-10).





(C)

**Fig. 1-11 Photograph images of EVA/SiO<sub>2</sub>-MPS nanocomposites (a) EVA/SiO<sub>2</sub>-MPS-T-3, (b) EVA/SiO<sub>2</sub>-MPS-T-5 and (c) EVA/SiO<sub>2</sub>-MPS-T-10**

The excellent dispersibility of MPS coated-SiO<sub>2</sub> into EVA was definitely shown in Fig. 1-12. In case of EVA/SiO<sub>2</sub>-oleate nanocomposite (Fig. 1-12 (a)), oleate could not make the reactivity between silica and EVA stronger. Therefore silica sank to bottom of EVA during the evaporation of xylene whereas hydrophobic and -S- group in MPS could enhance compatibility between EVA and SiO<sub>2</sub>. So it enabled SiO<sub>2</sub> to be finely dispersed into EVA (Fig. 1-12 (b)). Finally we decided to conduct mechanical property test with EVA/SiO<sub>2</sub>-MPS nanocomposite.

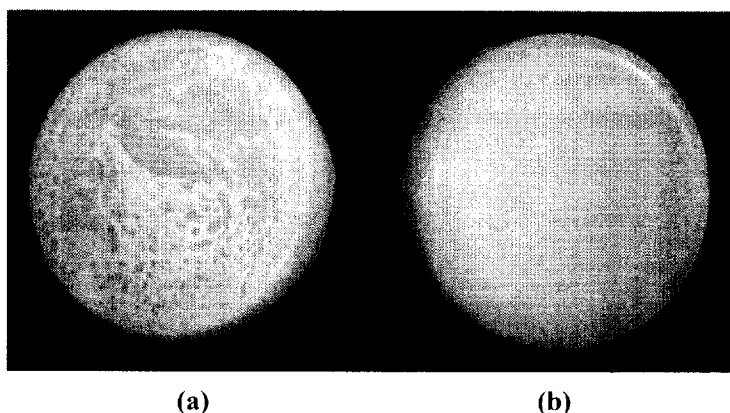


**Fig. 1-12 Photograph images of (a) EVA/SiO<sub>2</sub>-oleate-T-3 and (b) EVA/SiO<sub>2</sub>-MPS-T-3**

### 3.4. Mechanical property test of EVA/SiO<sub>2</sub>-MPS nanocomposite

#### 3.4.1. Selection of raw EVA

We had to select EVA which has either 12% or 18% VA contents. So we conducted abrasion test of EVA12-SiO<sub>2</sub>-T-3 and EVA18-SiO<sub>2</sub>-T-3 (Fig. 1-13). X axis indicates abrasion (mm) per regular polishing. EVA having 18% VA contents shows less abrasion (mm) than 12%. So we selected 18% VA contents which has good abrasion resistance. We prepared EVA/SiO<sub>2</sub>-MPS nanocomposite by using EVA having 18% VA contents for followed mechanical test.

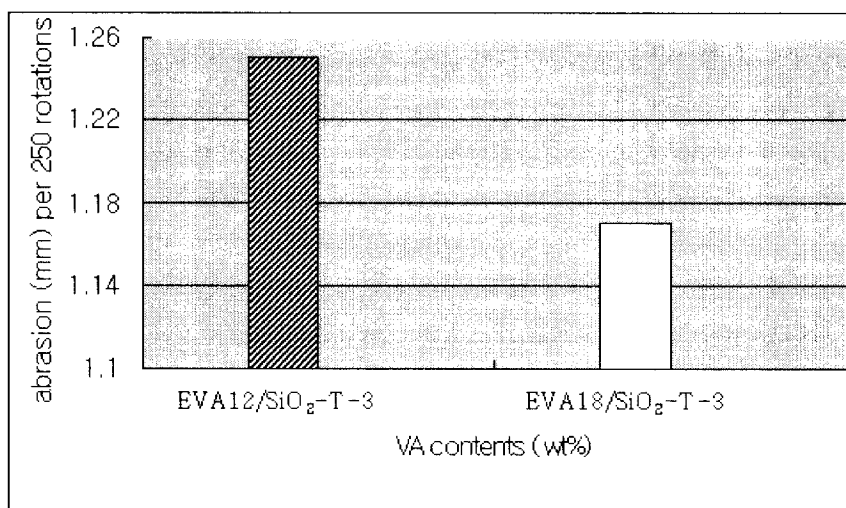


**Fig. 1-13 Abrasion resistance data of EVA12/SiO<sub>2</sub>-T-3 and EVA18/SiO<sub>2</sub>-T-3**

#### 3.4.2. Abrasion resistance test of EVA/SiO<sub>2</sub>-MPS nanocomposite

Fig. 1-14 shows results of abrasion test. By inserting MPS coated-SiO<sub>2</sub> into EVA, abrasion resistance was sharply improved. EVA18-SiO<sub>2</sub>-T-5 shows increase of abrasion resistance more than 300% compared with raw EVA. EVA18-SiO<sub>2</sub>-T-3 and EVA18-SiO<sub>2</sub>-M-3 also show an improved abrasion resistance more than 100%. The MPS surface treatments remove silanol groups and introduce new functional groups on silica surfaces, which can react with the polymer. The surface characteristics of silicas after MPS treatments lead to an increase of the

crosslink density of the EVA/silica composites<sup>12, 13</sup>. Therefore, abrasion resistance can increase.

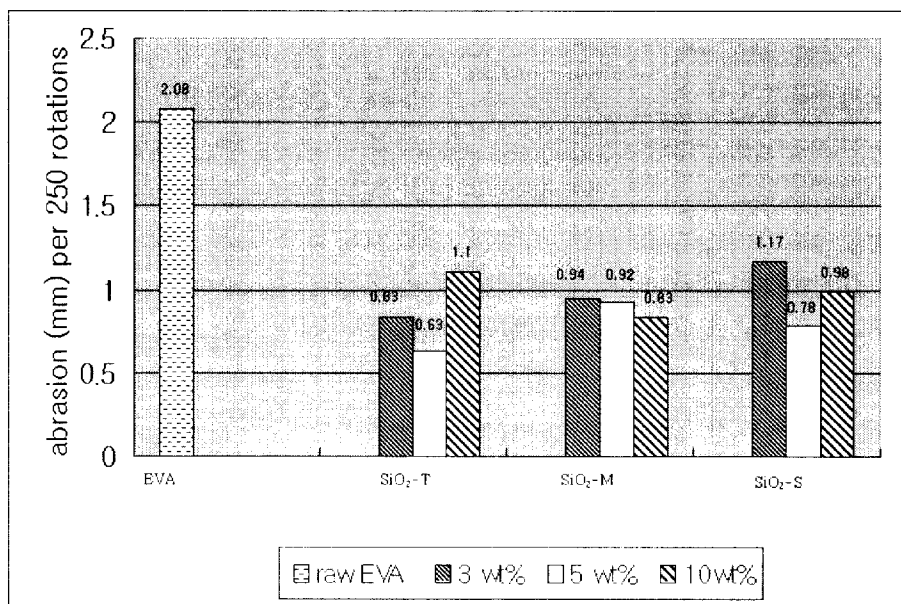


**Fig. 1-14 Abrasion resistance data of EVA18 and EVA18/SiO<sub>2</sub>-T-3, -T-5, -T-10 and EVA18/SiO<sub>2</sub>-M-3, -M-5, -M-10 and EVA18/SiO<sub>2</sub>-S-3, -S-5, -S-10**

### 3.4.3. Hardness test of EVA/SiO<sub>2</sub>-MPS nanocomposite

In Fig. 1-15, EVA-SiO<sub>2</sub>-T-5, and T-10 are improved as 7 Hs in hardness and EVA-SiO<sub>2</sub>-T-3 and M-3 show increase of 5 to 6 Hs in comparison with raw EVA.

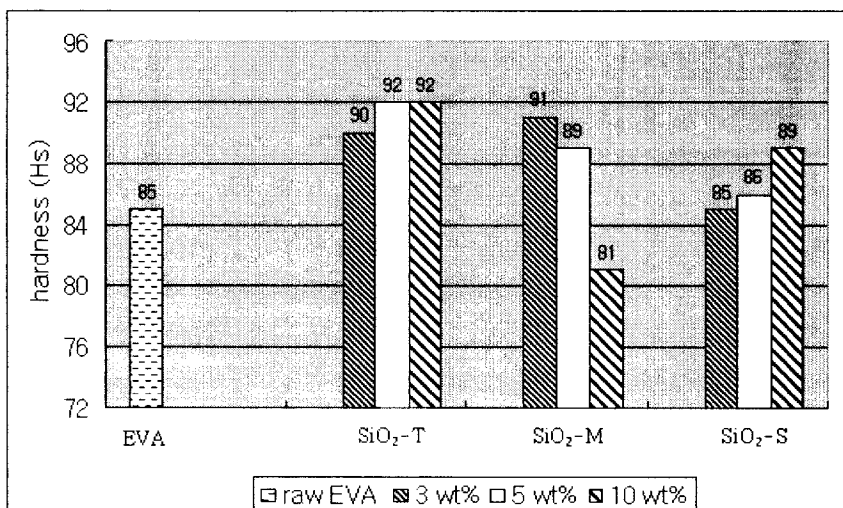


**Fig. 1-15 Hardness data of EVA18 and EVA18/SiO<sub>2</sub>-T-3, -T-5, -T-10 and EVA18/SiO<sub>2</sub>-M-3, -M-5, -M-10 and EVA18/SiO<sub>2</sub>-S-3, -S-5, -S-10**

#### 3.4.4. Tensile strength and elongation measurement of EVA/SiO<sub>2</sub>-MPS nanocomposite

We investigated tensile strength and elongation in order to confirm whether inserting SiO<sub>2</sub> nanoparticles into EVA has a bad influence upon original mechanical properties of EVA or not. Fig. 1-16 shows result of tensile strength. When SiO<sub>2</sub> nanoparticles inserted into EVA at the ratio of 3 wt%, they barely changed tensile strength in comparison with raw EVA. Therefore EVA-SiO<sub>2</sub>-T-3, M-3 and S-3 are better composite than others. In case of elongation measurement (Fig. 1-17), EVA-SiO<sub>2</sub>-M-3 barely changed elongation of original EVA.

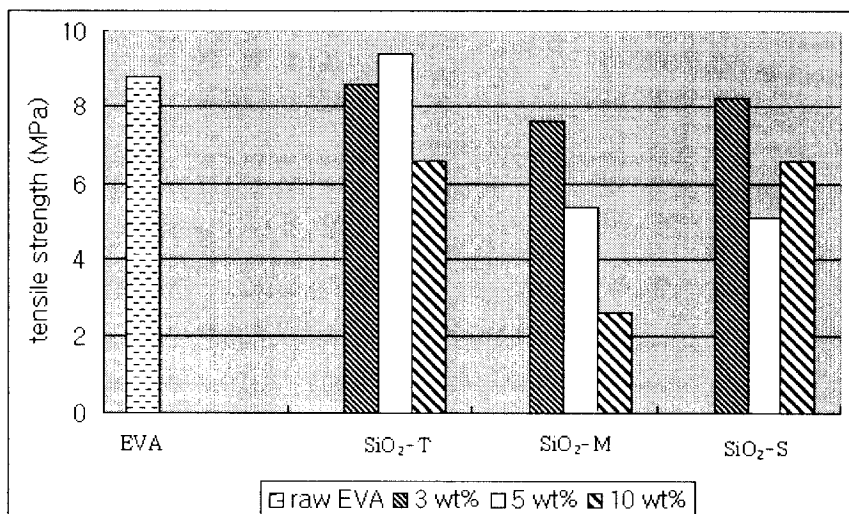


**Fig. 1-16 Tensile strength data of EVA18 and EVA18/SiO<sub>2</sub>-T-3, -T-5, -T-10 and EVA18/SiO<sub>2</sub>-M-3, -M-5, -M-10 and EVA18/SiO<sub>2</sub>-S-3, -S-5, -S-10**

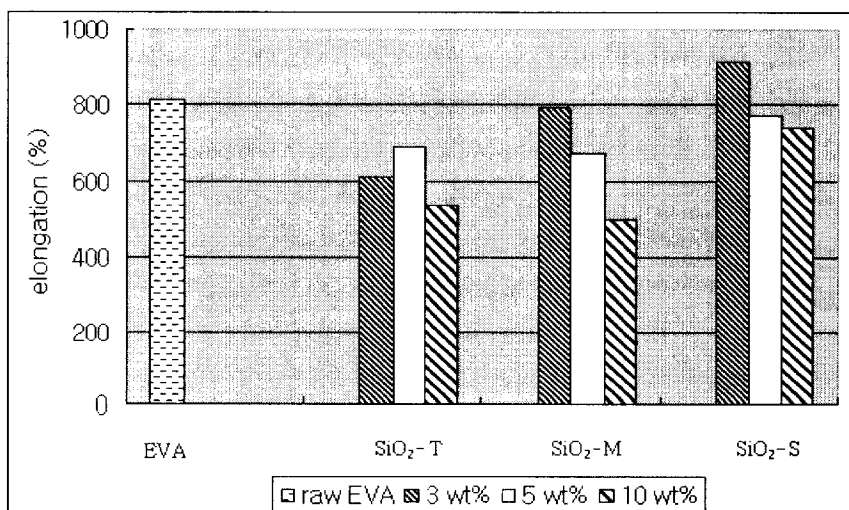


**Fig. 1-17 Elongation data of EVA18 and EVA18/SiO<sub>2</sub>-T-3, -T-5, -T-10 and EVA18/SiO<sub>2</sub>-M-3, -M-5, -M-10 and EVA18/SiO<sub>2</sub>-S-3, -S-5, -S-10**

#### 3.4.5. The most distinguished EVA/SiO<sub>2</sub>-MPS nanocomposite

We can conclude that EVA/SiO<sub>2</sub>-MPS nanocomposite has the best mechanical properties due to the highest dispersibility. EVA18-SiO<sub>2</sub>-T-3, 5 and EVA18-SiO<sub>2</sub>-M-3 were good in abrasion resistance. EVA18-SiO<sub>2</sub>-T-3, 5 and EVA18-SiO<sub>2</sub>-M-3 were good in hardness test. EVA18-SiO<sub>2</sub>-T-3, 5, EVA18-SiO<sub>2</sub>-M-3 and EVA18-SiO<sub>2</sub>-S-3 were barely changed in tensile strength. EVA18-SiO<sub>2</sub>-M-3, and EVA18-SiO<sub>2</sub>-S-3 were barely changed in elongation compared with raw EVA. EVA18-SiO<sub>2</sub>-M-3 shows distinguished value in all tests, It can have an improved abrasion resistance and hardness than raw EVA without changing tensile strength and elongation compared with raw EVA.

#### 4. Summary

We have successfully synthesized  $\text{SiO}_2$  nanoparticles by three methods from TEOS, sodium metasilicate and sodium silicate by emulsion route. Surface modification of the obtained  $\text{SiO}_2$  nanoparticles was done with oleic acid and MPS to enhance dispersion property and stability of silica surface. The obtained  $\text{SiO}_2$  nanoparticles were inserted into EVA at ratio of 3 wt%, 5 wt% and 10 wt%. By observation of photograph images, in case of EVA/ $\text{SiO}_2$ -oleate nanocomposite at ratio of all wt% of  $\text{SiO}_2$ -oleate, a great number of particles were aggregated. On the other hand, when it comes to EVA/ $\text{SiO}_2$ -MPS nanocomposites, they were perfectly dispersed into EVA therefore we conducted mechanical property tests with EVA/ $\text{SiO}_2$ -MPS nanocomposite. Consequently we confirmed the improved mechanical properties of EVA/ $\text{SiO}_2$ -MPS nanocomposite in abrasion resistance and hardness test without changing tensile strength and elongation compared with raw EVA. Especially EVA18- $\text{SiO}_2$ -M-3 shows the most improved value in all tests.

## 5. References

1. Bogush, G. H.; Tracy, M. A. and Zukoski IV, *Journal of Non-Crystalline Solids*, 104 (1988) 95.
2. Bogush, G. H.; Zukoski, C. F., *Journal of Colloid and Interface Science*, 1991, 141, 19.
3. Gmachowski, L., *Journal of Colloid and Interface Science*, 1996, 178, 80.
4. Osseo-Asare, K. and Arriagada, F. J., *Colloids and Surfaces*, 1990, 50, 321.
5. Gan, L. M.; Zhang, K. and Chew, C. H., *Colloids and Surfaces*, 1996, 110, 199.
6. Catauro, M.; Raucci, M. G.; De Gaetano, F. and Marotta, A., *Journal of Materials Science*, 2003, 38, 3097.
7. Rao, A. V.; Kalesh, R. R. and Pajonk, G. M., *Journal of Materials Science*, 2003, 38, 4407.
8. Walcarius, Alain.; Etienne, M. and Bessiere, J., *Chem. Mater.*, 2002, 14, 2757.
9. Y. Xia, B. Gates, Y. Yin and Y. Lu, *Adv. Mater*, 12, 10 (2000).
10. Apel, C.; Jordan, R. and Unger, K. K., *HPLC 1995*, Innsbruck, Austria
11. Kaiser, C.; Hanson, M.; Giesche, H.; Kinkel, J. and Unger, K. K., *Fine Particles Science and Technology*, 1996, 71.
12. Morris, R. M.; Klabunde, K. J., *Inorg. Chem.* 1983, 22, 682.
13. Bellobono, I. R.; Castellano, L.; Tozzi, A., *Mater. Chem. Phys.* 1991, 28, 69.
14. A. M. Salvi, R. Pucciariello, M. R. Guascito, V. Villani, L. Intermite, *Surf. Interface Anal.*, 2002, 33, 850.

15. A. P. Mathew, S. Packirisamy, S. Thoms, *Polum. Degrad. Stab.*, 2001, 72, 423
16. Teichner, S. J.; Nicolaon, G. A.; Vicarini, M. A.; Gardes, G. E. E. *Advances in Colloid and Interface Science* 1976, 5, 245.
17. Harris, M. R.; Sing, K. S. W. *J. Appl. Chem.* 1958, 8, 586.
18. Vicarini, Mo A.; Nicolaon, G. A.; Teichner, S. J. *Bull. Soc. Chim. Fr.* 1969, 196.
19. Gan, L. M.; Zhang, K.; Chew, C. H. *Colloids and Surfaces A: Physicochemical and Engineering Aspects* 1996, 110, 199.
20. Joshi, N.; Sakhalkar, S.; Hirt, D. the Annual Meeting of the Society of Plastics Engineers '96 proceeding, 1996, 2327.
21. Morris, R. M.; Klabunde, K. J. *Inorg. Chem.* 1983, 22, 682.
22. Bellobono, I. R.; Castellano, L.; Tozzi, A. *Mater. Chem. Phys.* 1991, 28, 69.
23. Bellobono, I. R.; Selli, E.; Righetto, L. *Mater. Chem. Phys.* 1988, 19, 131.
24. Fukude, Y.; Tanabe, K. *Bull. Chem. Soc. Jpn.* 1973, 46, 1616.
25. Beruto, D.; Botter, R.; Searcy, A. W. *J. Phys Chem.* 1984, 88, 4052.

## 6. Korean abstract

SiO<sub>2</sub> 나노입자는 TEOS (tetraethyl orthosilicate), sodium metasilicate와 sodium silicate로부터 합성되었다. SiO<sub>2</sub> 나노입자와 EVA (ethylene vinylacetate)와의 상용성과 분산성을 극대화 시키기 위해 실란 커플링제의 한 종류인 MPS (3-mercaptopropyl trimethoxysilane)으로 SiO<sub>2</sub> 나노입자를 표면코팅하였다. 나노입자의 형태와 분산성은 투과전자현미경(TEM), 주사전자현미경(SEM)으로 관찰하였고 나노입자의 표면코팅으로 인한 구조변화 및 성공적인 코팅을 푸리에변환 적외선분광분석기로 확인하였다. EVA/나노입자 복합체의 분산성은 광학사진으로 분석하였다. 최종적으로 EVA와 표면개질된 SiO<sub>2</sub> 나노입자와의 나노 복합체를 제조하여 내마모성, 경도, 인장강도와 신율 등의 기계적 특성을 조사하였다. EVA에 SiO<sub>2</sub> 나노입자가 도입됨으로 인해 내마모성과 경도는 현저하게 증가하였지만, 인장강도와 신율에 있어서는 미비한 감소가 있었다.

## **PART II**

### **Preparation of Heat Insulating Nanocomposite Film with MPS (mercaptopropyl trimethoxysilane) coated-Nanoparticles**

**Sung Woo Kim**

Research Advisor : Prof. Young Soo Kang

*Department of Chemistry, Graduate School, Pukyong National University*

#### **Abstract**

To improve the heat insulating property of plastic films, SiO<sub>2</sub> nanoparticles as inorganic insulating filler were prepared from sodium metasilicate by emulsion method in reverse micelle. MgO, Al<sub>2</sub>O<sub>3</sub> and CaO nanoparticles were also prepared. Surface modifications of synthesized heat insulating nanoparticles were accomplished with MPS (mercaptopropyl trimethoxysilane) coating to maximize homogeneous distribution and compatibility between obtained heat insulating nanoparticles and EVA (ethylene vinylacetate). Finally heat insulating films were prepared with MPS coated-heat insulating nanoparticles at the ratio of 2 wt% and EVA. The insulating capacity was tested by IR spectroscopy and light transmission was observed by UV-vis spectroscopy. The mechanical properties such as tensile strength, elongation, impact strength, tear strength, clarity and haze were also studied.

## 1. Introduction

Uniform silica microspheres in the micrometer and submicrometer size range are widely used in different areas. Beside the classical priority fields as support materials for chromatographic applications and polymer fillers further innovative applications appeared in the last years. Commercial applications of rubbers and plastics often require the use of particulate fillers to obtain the desired reinforcement. In the rubber industry, besides carbon blacks, silicas are the other reinforcing filler used to impart specific properties to rubber compounds<sup>1</sup>. Extensive work has also been carried out on structural development in silica/rubber composites<sup>2</sup>. The surface functional environment of silica particles is quite different from that of carbon blacks due to the existence of silanol groups in the particles. Thus, the primary discussion on the structural development in the silica/rubber system is focused on the interactions between silica particles and rubber molecules<sup>3</sup>. To maximize the interactions between silica and rubber, various methods used to modify the surface properties of the silicas are largely introduced in terms of thermal, chemical, electrochemical, and coupling agent treatments. Among them, silane coupling agents have been used in the rubber industry to improve the performance of silicas and other mineral fillers in rubber compounds. A silane coupling agent contains functional groups that can react with the rubber and the silicas. In this way, the rubber-silica adhesion is increased and consequently the reinforcing effect of the silicas is enhanced<sup>4, 5</sup>.

Nanocrystals of common metal oxides such as MgO, CaO and Al<sub>2</sub>O<sub>3</sub> have been shown to be highly efficient and active adsorbents for many toxic chemicals including air pollutants, chemical warfare agents, and acid gases<sup>6</sup>. Metal oxides are also an inorganic compound having very good heat resistance, thermal conductivity and alkali resistance. Magnesium oxide have been produced and utilized as filling agents in composite materials to achieve better mechanical strength, thermal shock resistance and thermal conductivity<sup>7</sup>. The transformation of Mg(OH)<sub>2</sub>, Ca(OH)<sub>2</sub> and Al(OH)<sub>3</sub> prepared from different precursors to the corresponding nanocrystals of metal oxides (MgO, CaO and Al<sub>2</sub>O<sub>3</sub>) that are insulating materials during thermal treatment was studied extensively in the past<sup>8-</sup>

In the light of these studies, we applied silane coupling agent modified-inorganic fillers (silicas,  $\text{Al}_2\text{O}_3$ ,  $\text{MgO}$  and  $\text{CaO}$ ) to filler-polymer nanocomposites as the reinforcing fillers which can improve mechanical properties and heat insulating ability in the insulating wavelength range (700–1,400 nm) of EVA (ethylene vinylacetate) film.

## 2. Experiments

### 2.1. Materials and Analytical Methods

Calcium (98.5%) from BDH Laboratory Supplies Poole, magnesium (98%), aluminium sec-butyrate (97%), sodium meta-silicate ( $\text{Na}_2\text{O} \cdot \text{SiO}_2 \cdot 9\text{H}_2\text{O}$ , Aldrich) and cyclohexane (> 99.5%) from Aldrich, polyoxyethylene nonylphenol ether (NP-5) and (NP-9) from IlChil Chemicals, were used as received. Ammonia solution ( $\text{NH}_4\text{OH}$ , Junsei), hydrochloric acid ( $\text{HCl}$ , Aldrich), MPS ( $\text{C}_6\text{H}_{16}\text{O}_3\text{SSi}$ , Aldrich) and EVA(ethylene vinylacetate), EF-443 from Hyundai Petrochemical Co. were used in their commercial form. Transmission electron microscopy (TEM) images were obtained by using a HITACHI, H-7500. X-ray powder diffraction (XRD) was obtained with a Philips, X'Pert-MPD system. Fourier Transform Infrared Spectroscopy (FTIR) spectra were obtained by using PERKIN ELMER SPECTRUM 2000. The tensile strength and elongation were measured with SHIMADZU, AG-10TG.

### 2.2. Syntheses of heat insulating nanoparticles by emulsion method

#### 2.2.1. Synthesis of nanosized- $\text{SiO}_2$ nanoparticles by emulsion method

Two types of inverse microemulsions, designated as microemulsion A (MA) and microemulsion B (MB), were first prepared separately. Both MA and MB contained two common components, i.e. a non-ionic surfactant mixture of NP-9 and NP-5 in a weight ratio of 2/3 and cyclohexane. The only difference was that MA consisted of an aqueous solution of sodium meta-silicate with 0.05 M concentration, while MB contained an aqueous solution of hydrochloric acid (0.05 M). MA contains cyclohexane of 68.10 wt%, NP-9/NP-5 (2/3) of 17.10 wt% and

an aqueous solution of sodium meta-silicate of 14.96 wt%. On the other hand, MB contains the same amount of cyclohexane and NP-9/NP-5 with MA except the aqueous solution of hydrochloric acid of 15.18 wt%. Equal amounts of the MA and MB microemulsions of those compositions were then mixed with continuous stirring at room temperature for about 2 hrs. The resulting mixed microemulsion was then destabilized by heating it up to about 80 °C. On cooling, it was separated into clear and turbid phases. The fine silica particles were recovered from the turbid phase by centrifugation. The particles were washed with acetone six times to remove residual surfactants. The silica particles were then dried at 100 °C in a vacuum oven.

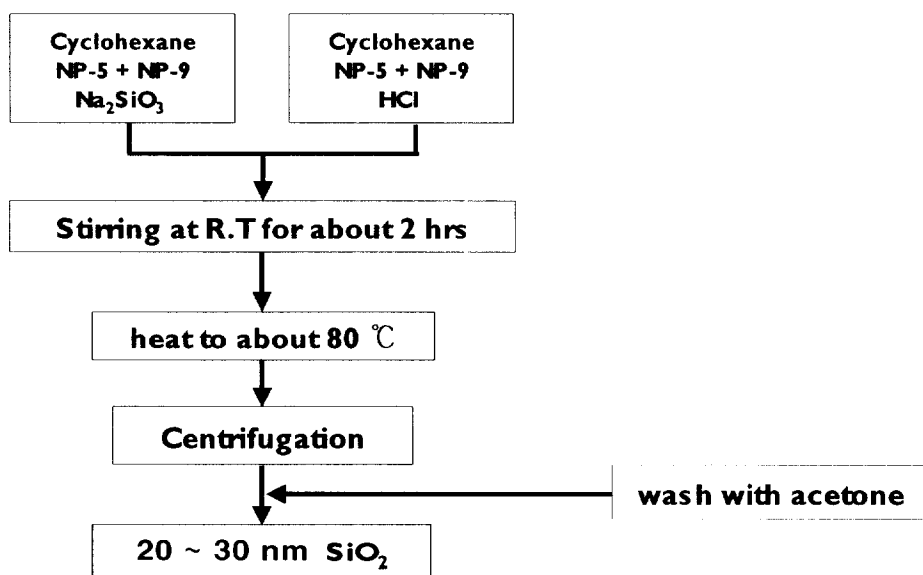


**Fig. 2-1 Schematic drawing of the synthetic process of nanosized-SiO<sub>2</sub> nanoparticles**

### 2.2.2. Synthesis of aggregated microsized-SiO<sub>2</sub> nanoparticles

The synthetic method of aggregated microsized-SiO<sub>2</sub> nanoparticles was followed as the same procedure in part I in Chapter 2.2.2.

### 2.2.3. Synthesis of $\text{Al}_2\text{O}_3$ nanoparticles

The principle of the preparation of alumina xerogels from aluminium alcoholates is known from the work of Adkins<sup>11</sup>. In order to apply to alumina aerogels a method similar to that proposed for silica, we selected aluminium sec-butyrate, a commercially available compound, which is soluble in sec-butanol<sup>12, 13</sup>. Aluminium hydroxide gel is precipitated from this solution at room temperature. The precipitation starts immediately after the first addition of water. Alumina aerogels were prepared from a 10% (by weight) solution in sec-butanol of aluminium sec-butyrate hydrolyzed by various quantities of water, the solvent being evacuated in the autoclave.

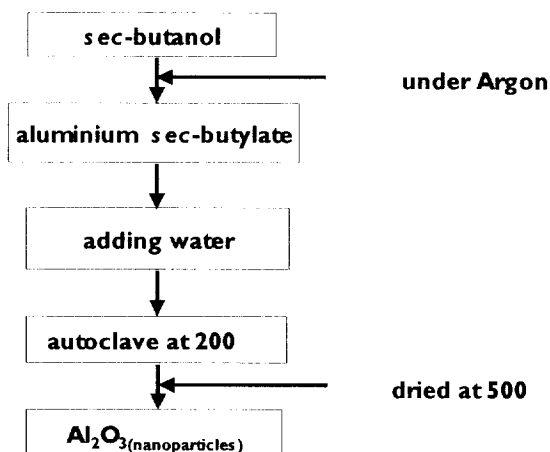


Fig. 2-2 Schematic drawing of the synthetic process of  $\text{Al}_2\text{O}_3$  nanoparticles

### 2.2.4. Synthesis of MgO and CaO nanoparticles

These methods are improved by adaptation of the previous reports<sup>8, 9</sup>. General procedures are described below for MgO and CaO<sup>9, 10</sup>. In a three-necked 2 L round bottom flask equipped with a mechanical stirrer, water cooled condenser, and argon inlet with a three-way stopcock was placed 300 mL of toluene. In another flask, 2.4 g (0.10 mol) of Mg turnings was allowed to react with 100 mL of  $\text{CH}_3\text{OH}$  under Ar. Then 4 mL (0.22 mol) of distilled water was added dropwise from a syringe over a 30 min period. This solution was stirred at room

temperature for 6 hrs under Ar. The resultant slightly milky solution (gel-like) was placed in an autoclave, heated to 200 °C, vented, and thus converted to a  $\text{Mg}(\text{OH})_2$  aerogel as previously described<sup>4</sup>. This fine white powder was heat treated (dehydrated) for 12 hrs under vacuum about 200 °C, and maintained at 500 °C in the electric furnace for overnight. CaO nanoparticle was prepared as the same procedures as described for MgO nanoparticle by using calcium metal.

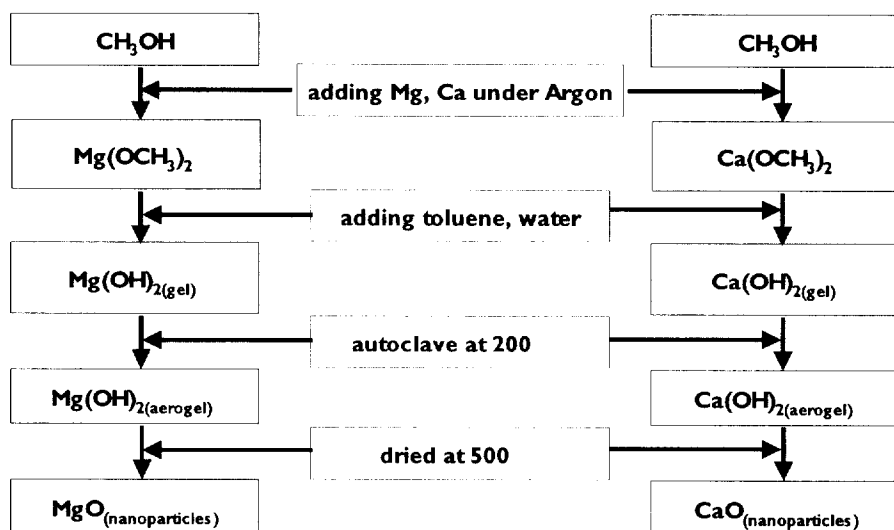


Fig. 2-3 Schematic drawing of the synthetic process of MgO and CaO nanoparticles

### 2.3. Surface modification of heat insulating nanoparticles

Surface modification of the obtained heat insulating nanoparticles was conducted with MPS by the same method as mentioned in Part I.

### 2.4. Preparation of EVA/heat insulating nanoparticle nanocomposite and EVA film with heat insulating ability by inserting surface modified-nanoparticles into EVA

EVA and surface modified-heat insulating nanoparticles which were added at the ratio of 2 wt% were well kneaded in Buss-Kneader. In this step, nanoparticles can be perfectly encapsulated by EVA, therefore nanoparticles were dispersed

separately without aggregation and strongly attached to EVA. Because MPS coated on nanoparticles avoided reversible aggregation of particles and maximized compatibility between nanoparticles and EVA. The kneaded composites were reformed as pellet type master batch by pelletizer and extruder. The insulating master batch was transferred into Blow Film Extruder in order to prepare heat insulating EVA film. Thickness of final film was controlled to obtain 60  $\mu\text{m}$ .

### 3. Results and discussion

#### 3.1. Nanosized-SiO<sub>2</sub> nanoparticles

Size of SiO<sub>2</sub> nanoparticles was determined as 20 ~ 30 nm by TEM image (Fig. 2-4). The particles are monodispersed and spherical which have narrow size distribution. The particles show spherical shape that may represent the simplest form that a colloidal particle can easily adopt during the nucleation or growth process, as driven by minimization of interfacial energy<sup>14, 15</sup>.



**Fig. 2-4 TEM image of nanosized-SiO<sub>2</sub> nanoparticles**

### 3.2. Al<sub>2</sub>O<sub>3</sub> nanoparticles

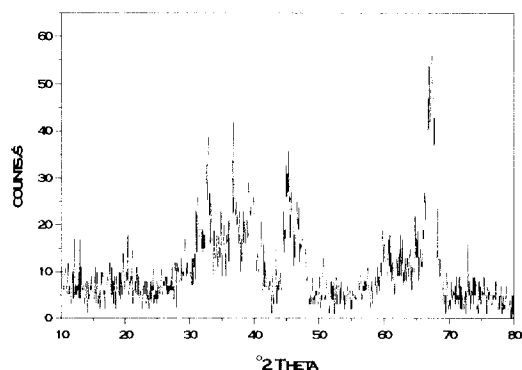


**Fig. 2-5 XRD spectrum of Al<sub>2</sub>O<sub>3</sub> nanoparticles**

The hexagonal crystalline structure of Al<sub>2</sub>O<sub>3</sub> was well matched with JCPDS card No. 03-0914. According to TEM image (Fig. 2-6), the particle shape is either spherical or oval with particle size of 10 ~ 20 nm.

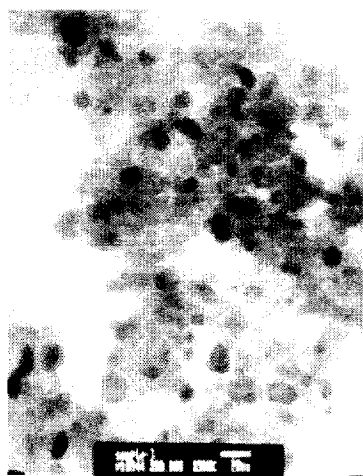


**Fig. 2-6 TEM image of Al<sub>2</sub>O<sub>3</sub> nanoparticles**

### 3.3. MgO nanoparticles

MgO with good crystallinity was matched with JCPDS card No. 77-2364 (Fig. 2-7). The particles show wide size distribution as 5 ~ 20 nm and are almost spherical (Fig. 2-8).

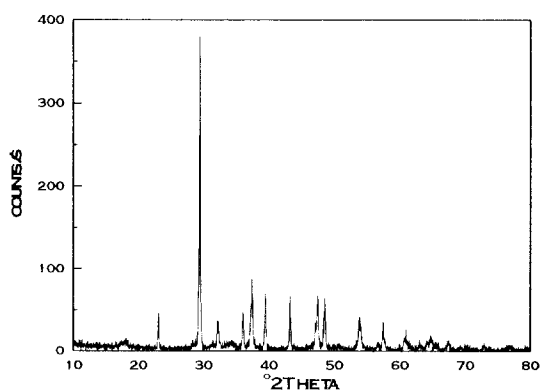


Fig. 2-7 XRD spectrum of MgO nanoparticles

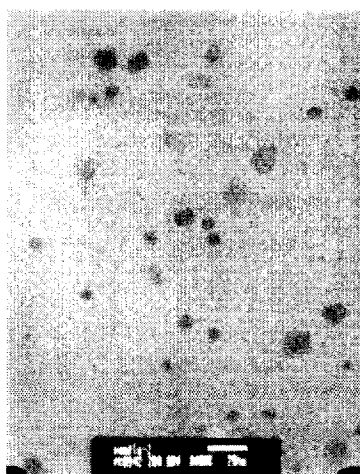
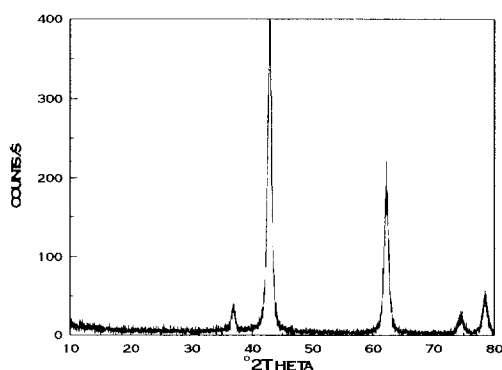


Fig. 2-8 TEM image of MgO nanoparticles

### 3.4. CaO nanoparticles

We determined that CaO nanoparticles were well matched with JCPDS card No. 77-2376 (Fig. 2-9). In TEM image (Fig. 2-10), the particles were neither monodispersed nor regular shape. Therefore, these particles have restrictions on applying to EVA films because these aggregated particles may reduce light transparency.



**Fig. 2-9 XRD spectrum of CaO nanoparticles**



**Fig. 2-10 TEM image of CaO nanoparticles**

### 3.5. Measurement of heat insulating property of surface modified-nanoparticles

To be used as heat insulating filler for EVA film, it should absorb radiated heat which has wavelength range of  $7\ \mu\text{m} \sim 10\ \mu\text{m}$  from ground during nighttime. The wavelength range of  $7\ \mu\text{m} \sim 10\ \mu\text{m}$  can be converted into the wavenumber range of  $700\ \text{cm}^{-1} \sim 1400\ \text{cm}^{-1}$  which indicates radiated heat. Therefore, heat insulating property of surface modified-nanoparticles can be indirectly measured by FT-IT spectra in the wavenumber range of  $700\ \text{cm}^{-1} \sim 1400\ \text{cm}^{-1}$ . In Fig. 2-11, MgO and CaO nanoparticles rarely absorbed the range of radiated heat, so it is concluded that they are not efficient heat insulating materials. On the other hand,  $\text{Al}_2\text{O}_3$  and  $\text{SiO}_2$  nanoparticles absorb the wavenumber range which is assumed as the same range of radiated heat.  $\text{Al}_2\text{O}_3$  shows heat insulating ability only at the range between  $700 \sim 950\ \text{cm}^{-1}$  however the value is negligible because of narrow range available.  $\text{SiO}_2$  nanoparticles which absorb the radiated heat throughout the range of  $700\ \text{cm}^{-1} \sim 1400\ \text{cm}^{-1}$  have the best heat insulating ability among the samples. The efficiency of heat insulating ability decreases according to the order of  $\text{SiO}_2 > \text{Al}_2\text{O}_3 > \text{CaO} > \text{MgO}$ .

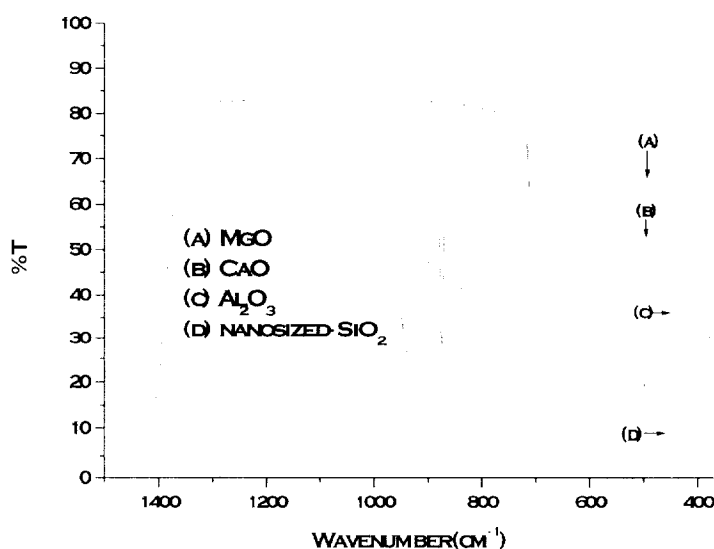
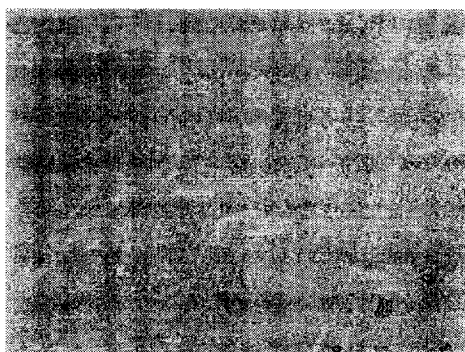


Fig. 2-11 FT-IR spectra of heat insulating nanoparticles

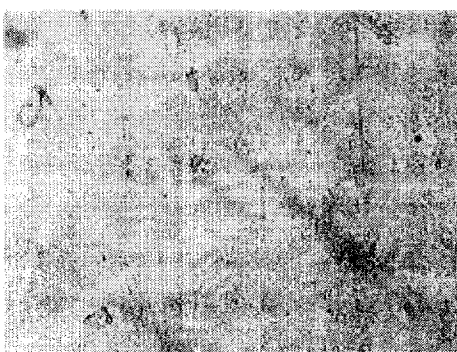
### 3.6. EVA/nanoparticles film with 60 $\mu\text{m}$ thickness

#### 3.6.1. Dispersibility of surface modified-nanoparticles in EVA

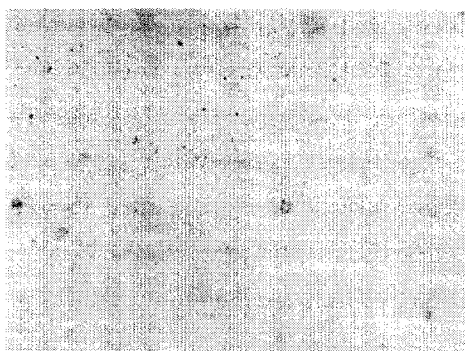
To investigate dispersibility of surface modified-nanoparticles in EVA, the images were obtained with optical microscope. In raw EVA film (Fig. 2-12), any alien substances were not observed however the films which contain heat insulating nanoparticles show some different things which is definitely surface modified-particles. EVA/ $\text{Al}_2\text{O}_3$ -MPS film represents film of 60  $\mu\text{m}$  thickness that is nanocomposite of EVA and MPS modified- $\text{Al}_2\text{O}_3$  nanoparticles. The other samples can be also described as the same manner for each heat insulating nanoparticles respectively. EVA/ $\text{Al}_2\text{O}_3$ -MPS film, EVA/ $\text{CaO}$ -MPS film and EVA/ $\text{SiO}_2$ -MPS (micro) film (Fig. 2-12 (b), (c), (f)) rarely show particles. Only few particles were observed and they even formed agglomerations. These results exactly correspond to their TEM images that show not monodispersed but aggregated particles. On the other hand, EVA/ $\text{MgO}$ -MPS film and EVA/ $\text{SiO}_2$ -MPS (nano) film (Fig. 2-12 (d), (e)) show excellent dispersibility of nanoparticles into EVA. In EVA/ $\text{MgO}$ -MPS film, MPS modified- $\text{MgO}$  particles were relatively well dispersed into EVA during preparing procedures of EVA film with the exception of few agglomerations. EVA/ $\text{SiO}_2$ -MPS (nano) film shows the best dispersibility without any agglomeration and as competitively low contents of 2 wt%, particles equally dispersed throughout EVA. Homogeneous distribution of nanosized- $\text{SiO}_2$  particles resulted from MPS coating onto silica surface. Nanosized- $\text{SiO}_2$  particles were monodispersed even before MPS modification. By coating MPS onto silica surface, reversible aggregation of particles was prevented and functional group, which can maximize compatibility between particles and EVA, attached to silica particles to make particles perfectly encapsulated in EVA. Therefore, we can conclude that successful MPS coating onto silica surface can lead to excellent EVA film with homogeneously monodispersed nanoparticles.



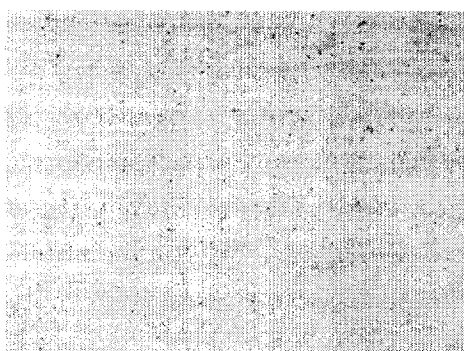
(a)



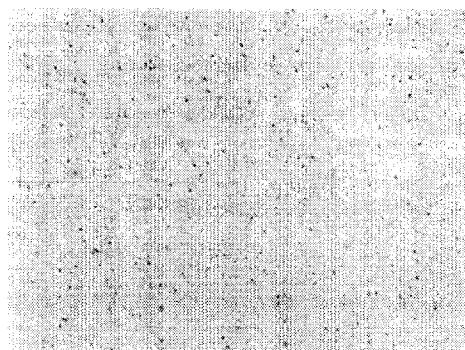
(b)



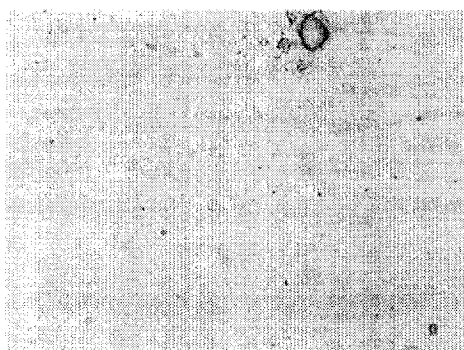
(c)



(d)



(e)



(f)

**Fig. 2-12 Optical microscope image of (a) EVA film, (b) EVA/Al<sub>2</sub>O<sub>3</sub>-MPS film, (c) EVA/CaO-MPS film, (d) EVA/MgO-MPS film, (e) EVA/SiO<sub>2</sub>-MPS(nano) film, (f) EVA/SiO<sub>2</sub>-MPS(micro) film**

### 3.6.2. Light transparency of EVA/nanoparticles film

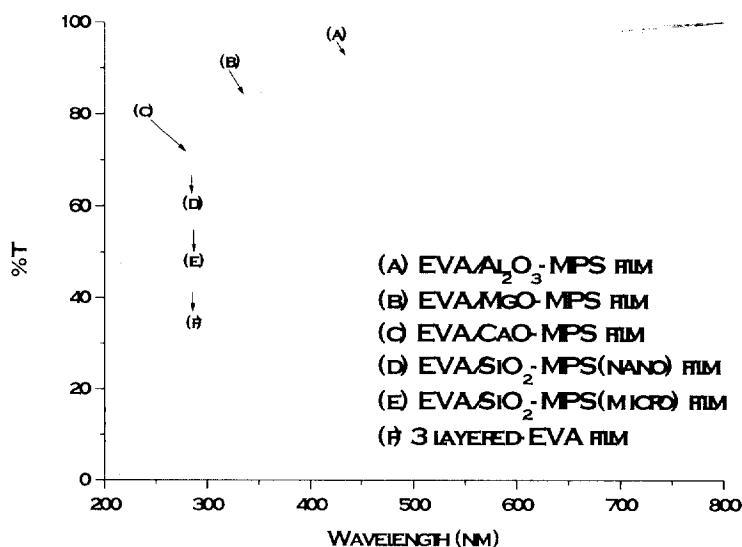


**Fig. 2-13 UV-vis spectra of EVA/nanoparticles film**

In addition to heat insulating property, one of the required fundamental properties of agricultural plastic film is light transparency in the daytime. Light which is useful at crop growth has the wavenumber range of 400 ~ 700 nm. Therefore, We can simply measure light transparency of plastic films with UV-vis spectra. In Fig. 2-13, 3 layered-EVA film which was receive from Ihl- Shin Chemical Co. in commercial form were used to compare it with the other prepared plastic films. All of the prepared films in this study show better light transparency compared with 3 layered-EVA. Vinyl films that include nanosized-particles have distinguished light transparency over 80% at the range of 400 ~ 700 nm because of low contents (2 wt%) of heat insulating filler and homogeneous distribution. Microsized-particle dispersed-film shows inferior property to in case of nanoparticles due to the lots of large agglomerations.

### 3.6.3. Measurement of heat insulating property of EVA/nanoparticles film

Heat insulating ability of plastic films was indirectly investigated by FT-IR spectra (Fig. 2-14). The plastic films which include MgO, CaO and  $\text{Al}_2\text{O}_3$  nanoparticles have low absorption ability as negligible value. These three films are not possible to be used as heat insulating film. 3 layered-EVA film, EVA/ $\text{SiO}_2$ -MPS(micro) film and EVA/ $\text{SiO}_2$ -MPS(nano) film show distinguished absorption ability over 50%. Especially, EVA/ $\text{SiO}_2$ -MPS(nano) film has the best heat insulating ability as 60%. It may act as efficient heat insulating film for agriculture. The efficiency of heat insulating ability increases according to the order of EVA/MgO-MPS film < EVA/CaO-MPS film < EVA/ $\text{Al}_2\text{O}_3$ -MPS film < 3 layered-EVA film < EVA/ $\text{SiO}_2$ -MPS(micro) film < EVA/ $\text{SiO}_2$ -MPS(nano) film.

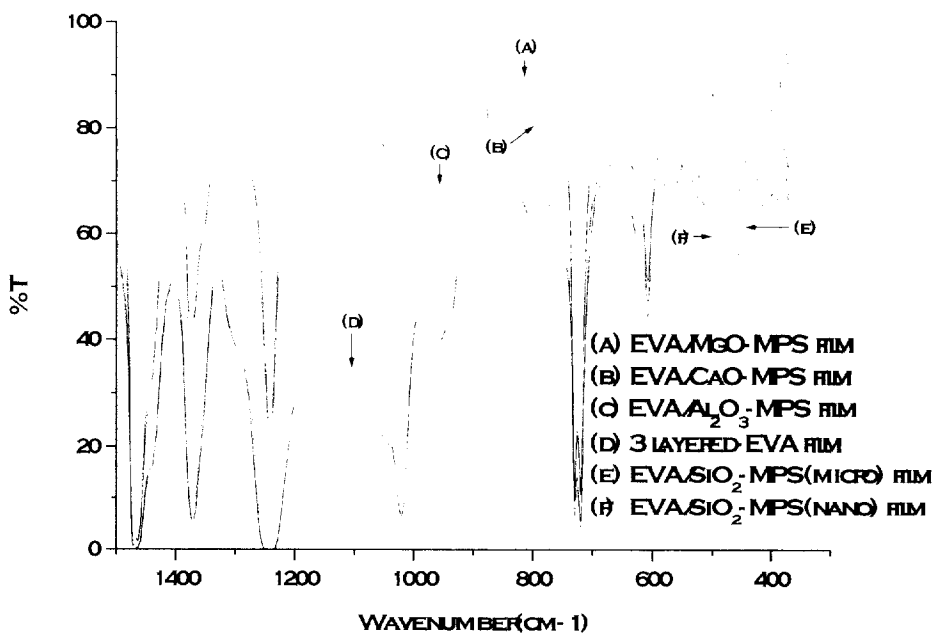


Fig. 2-14 FT-IR spectra of EVA/nanoparticles film

### 3.4. Mechanical property test for EVA/nanoparticles film

	thickness ( $\mu\text{m}$ )	tensile strength		elongation		tear strength		HAZE	
		( kg f/cm <sup>2</sup> )		( % )		( kg f/cm <sup>2</sup> )		( % )	
		TD	MD	TD	MD	TD	MD	Clarity	Haze
EVA(EF-443)	60	270	250	600	300	160	130		3.4
EVA/SiO <sub>2</sub> - MPS(micro) film	60	272	236	658	513	118	93	92.5	10.6
EVA/SiO <sub>2</sub> - MPS(nano) film	60	285	294	695	406	115	96	93.3	7.1

**Table. 2-1 Mechanical property test for EVA/nanoparticles film**

In this Chapter, we investigated mechanical properties of EVA/nanoparticles film in order to find out whether defect of mechanical properties might be occurred when nanoparticles were inserted into EVA. For this reason, the prepared nanocomposite EVA films were compared with raw EVA. We focus on making mention about nanocomposite films that contain SiO<sub>2</sub> nanoparticles because EVA/SiO<sub>2</sub>-MPS(micro) film and EVA/SiO<sub>2</sub>-MPS(nano) film showed excellent efficiency in heat insulating property and light transparency. From the measurement of tensile strength, EVA/SiO<sub>2</sub>-MPS(nano) indicated superior tensile strength to raw EVA film and the balance between TD and MD was also excellent. EVA/SiO<sub>2</sub>-MPS(micro) film has the equal value of tensile strength compared with raw EVA film. In the elongation measurement, by inserting MPS modified-SiO<sub>2</sub> nanoparticles into EVA, the value of elongation was remarkably improved. However, inserted nanoparticles had a bad influence upon tear strength, clarity and haze but the decreased value was little as it can be negligible. Furthermore, in spite of decrease, the values were even over quality standards for heat insulating film (Table. 2-2). It is prescribed in the quality standards for heat insulating film that tear strength should be satisfied over 60 kgf/cm<sup>2</sup> and the value of haze should meet below 25%. From these results, we can conclude that MPS coating on silica

surface has definitely positive effect on mechanical property with negligible decrease in clarity between silica and EVA by maximizing compatibility because the EVA-silica adhesion is increased and consequently the reinforcing effect of the silica is enhanced<sup>16, 17</sup>.

	Thickness (mm)			
	0.060	0.070	0.080	0.100
Tensile strength ( kgf/cm <sup>2</sup> )	over 160	over 170	over 170	over 180
Elongation (%)	over 220	over 220	over 220	over 270
Tear strength ( kgf/cm <sup>2</sup> )	over 60	over 60	over 60	over 70
Haze (%)	below 25			

**Table. 2-2 Quality standards for heat insulating film**

#### 4. Summary

Nanoparticles such as  $\text{SiO}_2$ ,  $\text{MgO}$ ,  $\text{CaO}$  and  $\text{Al}_2\text{O}_3$  which have absorbing ability of radiated heat between 800 and 1400 nm range were successfully prepared. Surface modification of obtained insulating inorganic fillers was conducted by MPS (mercaptopropyl trimethoxysilane) that is a kind of silane coupling agents in order to enhance compatibility between EVA and inorganic fillers and attain perfect encapsulation of nanoparticles with EVA. Finally, to investigate dispersibility of nanoparticles in EVA, heat insulating property, light transparency and mechanical properties such as tensile strength, elongation, tear strength and haze, EVA/surface modified-nanoparticles films with 60  $\mu\text{m}$  thickness were prepared with Blow Film Extruder. MPS modified nanosized- $\text{SiO}_2$  and  $\text{MgO}$  nanoparticles showed distinguished dispersibility in EVA. Once monodispersed spherical nanoparticles are prepared, the dispersibility of particles are kept. Because MPS grafting onto silica surface can prevent irreversible aggregation of particles. On the other hand, because  $\text{Al}_2\text{O}_3$ ,  $\text{CaO}$  and micro-sized- $\text{SiO}_2$  were not prepared with monodispersed shape, in spite of MPS modification, the particles were not dispersed separately into EVA. Light transparency was simply measured with UV-vis spectrophotometer. All of the prepared nanocomposite films that include nanosized-particles have distinguished light transparency over 80% at the range of 400 ~ 700 nm because of low contents (2 wt%) of heat insulating filler and homogeneous distribution. Micro-sized-particle dispersed- film shows inferior property to those of nanoparticles due to the lots of large agglomerations. Heat insulating ability of films was indirectly investigated by FT-IR spectra. Especially, EVA/ $\text{SiO}_2$ -MPS(nano) film has the best heat insulating ability as 60%. It may act as efficient heat insulating film for agriculture. The efficiency of heat insulating ability increases according to the order of EVA/ $\text{MgO}$ -MPS film < EVA/ $\text{CaO}$ -MPS film < EVA/ $\text{Al}_2\text{O}_3$ -MPS film < 3 layered-EVA film < EVA/ $\text{SiO}_2$ -MPS(micro) film < EVA/ $\text{SiO}_2$ -MPS(nano) film. We investigated mechanical properties of EVA/nanoparticles film in order to find out whether defect of mechanical properties might be occurred when nanoparticles were inserted into EVA. From the measurement of tensile strength, EVA/ $\text{SiO}_2$ -MPS(nano) indicated superior

tensile strength to raw EVA film. In the elongation measurement, by inserting MPS modified-SiO<sub>2</sub> nanoparticles into EVA, the value of elongation was remarkably improved. Clarity and haze measurements show decreased value that is little as it can be negligible. We can conclude that MPS coating on silica surface has definitely positive effect on mechanical property with negligible decrease in clarity between silica and EVA by maximizing compatibility.

## 5. References

1. Gent, A. N.; Wang, C., J. Polym. Phys., 1996, 34, 2231.
2. Park, S. J.; Donnet, J. B., J. Colloid Interface Sci., 1998, 206, 29.
3. Mele, P.; Marceau, S.; Brown, D.; Puydt, Y.; Alberola, N. D., Polymers, 2002, 43, 5577.
4. Cheng, J.; Fone, M.; Ellsworth, M., Solid State Nucl. Magn. Reson., 1996, 7, 135.
5. De Boer, J. H.; Lippens, B. C.; Lisnsen, B. G.; Broekhoff, J. C. P.; Heuvel, A.; Osinga, T. V., J. Colloid Interface Sci., 1966, 21, 405.
6. Klabunde, K. J.; Stark, J. V.; Koper, O. B.; Mohs, C.; Park, D. G.; Decker, S.; Jiang, Y.; Lagadic, I.; Zhang, D., J. Phys. Chem. 1996, 100, 12142.
7. Lee, J. D.; Concise Inorganic Chemistry, 5th ed., Chapman and Hall, New York, pp. 339.
8. Utamapanya, S.; Klabunde, K. J.; Schlup, J. R., Chem. Mater., 1991, 3, 175.
9. Morris, R. M.; Klabunde, K., J. Inorg. Chem., 1983, 22, 682.
10. Klabunde, K. J.; Stark, J.; Koper, O.; Mohs, C.; Park, D. G.; Decker, S.; Jiang, Y.; Lagadic, I.; Zhang, D. J., J. Phys. Chem., 1996, 100, 142.
11. Adkins. A.; Amer. J., Chem. Soc. 1922, 44, 2175.
12. Teichner, S. J.; Nicolaon, G. A.; Vicarini, M. A.; Gardes, G. E. E. Advances in Colloid and Interface Science 1976, 5, 245.
13. Harris, M. R.; Sing, K. S. W. J. Appl. Chem. 1958, 8, 586.
14. Matijevic, E., Acc. Chem. Res., 1981, 14, 22.
15. Matijevic, E., Chem. Mater., 1993, 5, 412.

16. Morris, R. M.; Klabunde, K., *J. Inorg. Chem.*, 1983, 22, 682.
17. Cheng, J.; Fone, M. and Ellsworth, M., *Solid State Nucl. Magn. Reson.*, 1996, 7, 135.
18. De Boer, J. H.; Lippens, B. C.; Lisnsen, B. G.; Broekhoff, J. C. P.; Heuvel, A. and Osinga, T. V., *J. Colloid interface Sci.*, 1966, 21, 405.
19. Fukude, Y.; Tanabe, K. *Bull. Chem. Soc. Jpn.*, 1973, 46, 1616.
20. Beruto, D.; Botter, R.; Searcy, A. W. *J. Phys Chem.* 1984, 88, 4052.
21. Philipp, R.; Fujimoto, K. *J. Phys. Chem.* 1992, 96, 9035.
22. Philipp, R. P.; Omata, K.; Aoki, A.; Fujimoto, K. *J. Catal.* 1992, 34, 422.
23. Mizushima, Y.; Hori, M. *Appl. Catal.* 1992, A88, 137.
24. Mizushima, Y.; Hori, M. *J. Non-Cryst. Solids* 1994, 167, 1
25. Yoshida, A. *Adv. Chem. Ser.* 1994, 234, 51.
26. Innes, W. B. In *Experimental Methods in Catalytic Research*; Anderson, R. B., Ed.; Academic Press: New York, 1968; p 44.
27. Warren, B. E. *X-ray Diffraction*; Addison-Wesley: Reading, MA, 1969; p 21.
28. Mikhail, R. S.; Robens, E. *Microstructure and Thermal Analysis of Solid Surfaces*; Wiley: Chichester, 1983; Part 1.
29. G. H. Bogush, M. A. Tracy and Zukoski IV, *Journal of Non-Crystalline Solids*, 104, 95 (1988).
30. G. H. Bogush and C. F. Zukoski, *Journal of Colloid and Interface Science*, 142, 19 (1991).
31. Y. Xia, B. Gates, Y. Yin and Y. Lu, *Adv. Mater.*, 12, 10 (2000).

## 6. Korean abstract

농업용 필름의 한가지 기능은 야간에 지면으로부터 방사되는  $7\ \mu\text{m} \sim 10\ \mu\text{m}$ 의 파장대를 가지는 방사에너지(열)를 흡수하는 것이다. 보온필름은 방사열을 흡수하여 주간과 야간의 비닐하우스 내부의 온도차이를 최소화하여 냉해를 방지해야 한다. 농업용 필름에 보온성을 부여하기 위해 보온성 filler로써  $\text{SiO}_2$ ,  $\text{Al}_2\text{O}_3$ ,  $\text{MgO}$  와  $\text{CaO}$  나노입자를 합성하였고, EVA (ethylene vinylacetate) 와 나노입자와의 상용성 및 분산성을 극대화하기 위해 MPS (mercaptopropyl trimethoxysilane) 로 나노입자의 표면을 개질시켜 나노입자의 표면에 고분자와 결합을 이룰 수 있는 관능기를 도입하였다. EVA에 나노입자를 2 wt%의 중량비로 혼합하여 펠렛타이저에서 마스터배치를 제조한 후 Blow Film Extruder를 이용하여  $60\ \mu\text{m}$  두께의 필름을 제조하였다. 보온성 무기 filler ( $\text{SiO}_2$ ,  $\text{Al}_2\text{O}_3$ ,  $\text{MgO}$  와  $\text{CaO}$  나노입자)를 함유한 EVA 필름의 분산성은 광학현미경으로 관찰하였고, 광 투과도는 자외선-가시광선 분광분석기로 분석하였다. 보온성은 간접적인 방법으로 적외선 분광분석기로  $700\ \text{cm}^{-1} \sim 1400\ \text{cm}^{-1}$ 의 흡수율로 확인하였다. EVA에 나노입자가 도입됨에 따라 물성저하가 일어나는지 조사하기 위해 광 투과도와 보온성에서 우수한 특성을 보인 나노크기의  $\text{SiO}_2$ 를 함유한 필름과 마이크로 크기의  $\text{SiO}_2$ 를 함유한 필름의 인장강도, 신율, 인열강도 및 탁도를 측정하였다. 나노입자가 2 wt%의 낮은 중량비로 혼합되었기에 EVA 고유의 물성에는 크게 저하를 일으키지 않았고 오히려 인장강도 및 신율에서 물성이 증가되었다. 인열강도 및 탁도에서는 물성저하가 일어났으나 미비한 정도였고 보온필름의 품질규격 수치를 능가하는 값이었다.